77-13,664

MILSTED, Amy, 1944-
THE STRUCTURE AND FORMATION OF THE MITOTIC SPINDLE OF DROSOPHILA MELANOGASTER BLASTEMA EMBRYOS.

City University of New York, Ph.D., 1977
Biology

THE STRUCTURE AND FORMATION OF THE MITOTIC SPINDLE OF *DROSOPHILA MELANOGASTER* BLASTEMA EMBRYOS

by

Amy Milsted

A dissertation submitted to the Graduate Faculty in Biology in partial fulfillment of the requirements for the degree of Doctor of Philosophy, The City University of New York.

1977

This manuscript has been read and accepted for the Executive Committee in Biology in satisfaction of the dissertation requirement for the degree of Doctor of Philosophy.

January [illegible], 1977
Date

William D. Cohen 1/6/77
Chairman of Examining Committee
Prof. Wm. D. Cohen

January 7, 1977
Date

Executive Officer
Prof. [illegible] Moriber

Prof. [illegible] Grant — Hunter College, Institution

Prof. [illegible] Kyser — Hunter College, Institution

Prof. [illegible] Jensen — Lehman College, Institution

Prof. [illegible] Schuster — Brooklyn College, Institution

Prof. [illegible] Tolfer — Institute for Basic Research in Mental Retardation, Institution

Prof. [illegible] Goldman — Mellon Institute, Carnegie-Mellon University, Institution

The City University of New York

Abstract

THE STRUCTURE AND FORMATION OF THE MITOTIC SPINDLE OF DROSOPHILA MELANOGASTER BLASTEMA EMBRYOS

by

Amy Milsted

Advisor: Professor William D. Cohen

Mitotic spindles in situ are surrounded by multiple layers of spindle-delimiting membranes throughout mitosis. At prophase a conspicuous region of tubular endoplasmic reticulum appears in association with both the spindle-delimiting membranes and with cytoplasmic membranes. A role for tubular ER and spindle-delimiting membranes in the control of Ca^{++} levels and in microtubule assembly and disassembly is suggested.

Hexylene glycol isolated spindles appear very fibrous, and their physiological responses are similar to those of similarly isolated spindles of other species.

An isolation medium which employs tubulin polymerization conditions was used to isolate spindles which preserve major in situ morphological characteristics of Drosophila spindles. In such isolated spindles, four major interzonal fibers are visible under phase contrast. This number may be significant since D. melanogaster has four pairs of chromosomes. Each interzonal fiber has a midbody at its midregion in anaphase. At telophase the four midbodies of anaphase apparently coalesce laterally into one large midbody, and only one interzonal fiber can be seen.

During all mitotic stages structures 0.7 μm in diameter are present at the position expected for centrioles. These are too large to be

accounted for by an individual centriole; they have been termed centriole complexes.

The scanning electron microscope (SEM) was used in order to obtain a three dimensional impression of whole isolated spindles. Methods were developed for following individual spindles through all steps of processing for the SEM. The SEM shows a progressively more ordered spindle framework developing from prophase through anaphase and telophase. Chromosomes have been identified on the spindle, and centriole complexes have been described. The centriole complex apparently consists of a centriole plus associated material, which itself has substructure. Attachment of the centriole complex to the rest of the mitotic apparatus is tenuous. Larger diameter spindle fibers are seen to be composed of smaller diameter fibrils arranged in bundles.

Thin sections through spindles isolated under tubulin polymerizing conditions verify the presence of midbodies in isolates. Midbodies are not obvious in the SEM. In this system, in which cytokinesis does not occur during the blastema stage of development, midbodies seem not to be directly involved in cytokinesis.

Using a flattened metaphase spindle viewed in the SEM, it is possible to estimate the amount of tubulin required to construct this spindle. Approximately $2.0 - 4.6 \times 10^{7}$ monomers of tubulin per spindle would be needed; therefore about $1.2 - 2.8 \times 10^{-8}$ gm per embryo would be enough to construct all the spindles present in the syncytial embryo at this stage. This data is in good agreement with that previously published for both numbers of monomers per spindle in other species and numbers of grams of tubulin per embryo in D. melanogaster.

Acknowledgements

I would like to express my deep appreciation to my sponsor, Dr. W. D. Cohen, for his continuing support and assistance during the course of this work. Without his suggestions and enthusiasm this project may not have been completed.

My advisory committee at Hunter College - Dr. K. M. Lyser and Dr. R. J. Grant - have also been most helpful.

In addition, I want to express my thanks to Dr. R. D. Goldman for his support and encouragement during the preparation of this thesis.

Many other people have also been of help, and I thank them all: Dr. I. R. Herskowitz, Dr. R. Sederoff, Dr. T. E. Jensen, Dr. E. de Harven, and N. Lampen.

Finally, I thank all my family and friends for their understanding and patience during this time.

TABLE OF CONTENTS

LIST OF PLATES

LIST OF FIGURES

I. Introduction

The structure of mitotic and meiotic spindles has been examined in many diverse species, both in situ (for example, Schrader, 1953; Harris, 1962; Roth and Daniels, 1962; Robbins and Jentzch, 1969; Bajer and Molé-Bajer, 1969) and after isolation (Rebhun and Sharpless, 1964; Kane, 1962; Müller, 1970; Forer and Zimmerman, 1974; Rebhun, Rosenbaum, Lefebvre and Smith, 1974). The major structural elements common to all spindles studied to date are microtubules, and spindle organization, function and control are probably based at least partly upon the properties of spindle microtubules and cellular control over them.

Various techniques have been used to study spindle structure, including thin sectioning (Kane, 1962; Goldman and Rebhun, 1969; Cohen and Gottlieb, 1971; McIntosh and Landis, 1971; Brinkley and Cartwright, 1971; Fuge, 1973) and negative staining for transmission electron microscopy (TEM) (Kiefer et al., 1966), high voltage transmission electron microscopy (McIntosh et al., 1975) and phase contrast, polarizing and interference light microscopy (Kane and Forer, 1965; Rebhun and Sander, 1967; Cohen, 1968; Forer and Goldman, 1972; Inoué, Borisy and Kiehart, 1974; Salmon, 1975). During the course of the work described here, scanning electron microscopy (SEM) has also been employed in order to provide new information on isolated spindle organization and structure (Milsted, Cohen and Lampen, 1977). The abbreviation SEM will refer here to both scanning electron microscopy and the scanning electron microscope; similarly, the abbreviation TEM will be applied to both transmission electron microscopy and the transmission electron microscope.

The traditional method used in three dimensional reconstruction

of a spindle has been serial thin sectioning through whole mitotic cells (McIntosh and Landis, 1971; Brinkley and Cartwright, 1971; Tippit, McDonald and Pickett-Heaps, 1975). This method is extremely tedious and time consuming, and it limits the number of spindles which can be examined in this way. High voltage transmission electron microscopy of 1 μm thick sections (McIntosh et al., 1975), while enabling the viewer to examine an entire serially thick sectioned spindle in relatively few sections, is not routinely available. Negative staining of large spindles, such as those of sea urchin zygotes (Kiefer et al., 1966) is not a good method for demonstrating spindle fine structure, although it might be useful for examining smaller spindles of relatively simple structure.

Scanning electron microscopy, in comparison with the above methods which use transmitted electrons, allows great depth of field and direct three-dimensional imaging of objects, permitting visualization of general structural organization in but one or a few micrographs. SEM has recently been applied to the study of organelles, and it is of most value in the case of structures too large or too thick for TEM whole mounts (Kersey and Wessells, 1976; Kirschner, Rusli and Martin, 1975). Isolated mitotic spindles can be included in this category; with appropriate preparation methods there should be no surrounding membranes or other material obscuring the view of the spindles' fibrous structure. In order to make use of the advantages offered by SEM, spindles must necessarily be isolated and free of adhering cytoplasmic debris.

Although numerous spindles from widely varied species have been examined with many different methods, the manner in which the mitotic

apparatus functions is not clearly understood. A number of models have been proposed to explain chromosome movement and spindle elongation; (a) polymerization and depolymerization of spindle microtubules has been suggested by Inoué (1960; Inoué and Sato, 1967); (b) a sliding filament theory of chromosome movement postulates movement of microtubules along each other and in some cases apparent crossbridges have been seen between adjacent microtubules (McIntosh, Hepler and Van Wie, 1969; Hepler, McIntosh and Cleland, 1970); (c) a "zipper" hypothesis has been proposed by Bajer (1973), and (d) actomyosin-like mechanisms have also been suggested (Rebhun, 1967; Forer, 1969, 1974). There has long been evidence accumulating that there might be oriented components in addition to microtubules which contribute to spindle fiber birefringence (Forer, 1966; Goldman and Rebhun, 1969; Forer and Goldman, 1972; Forer, 1974). Actin-like microfilaments might be one other component. Other studies using polarized light indicate that all spindle birefringence is due to microtubules alone, however (Inoué and Sato, 1967).

Spindle isolation has been a major approach to the study of morphology and chemistry of spindles. Isolated spindles, free of obscuring cytoplasm and interfering cytoplasmic fluids and structures such as membranes and ribosomes, have served as simplified systems for the study of the mitotic apparatus, with the advantage that experimental conditions can be altered by changing the defined medium in which the spindles are bathed. Usually spindles are not clearly seen in living cells, but after isolation they are readily visible under phase contrast. As a consequence, spindles of the desired stage and orientation can be selected and their structural and physiological properties studied. Squash preparations of mitotic cells and embryos lend themselves to studies involving media variables such as pH, since solutions can easily be

perfused between coverslip and slide in such a preparation. The ultimate spindle model would be one that functions after removal from a cell. Such a model has not yet been developed, although many attempts have been made, beginning with the work of Hoffman-Berling (1954).

Spindles were first isolated in 1952 by Mazia and Dan, who arrested division of sea urchin zygotes and stabilized the mitotic apparatus by fixing cells in cold ethanol, then selectively solubilized cells with digitonin; these alcohol-detergent isolated spindles were not very soluble (Mazia and Dan, 1952). Next came the first direct isolation of the mitotic apparatus by lysis of cells into a medium containing the disulfide reagent, dithiodiglycol (Mazia et al., 1961). Kane later showed that an -S-S- reagent is not necessary for isolation and used instead a penetrating non-electrolyte at pH 6.2 (Kane, 1962; 1965). Kane's hexylene glycol isolation medium was commonly used by many workers, and consisted of 12% hexylene glycol, 0.01 M potassium phosphate, pH 6.3, used for isolation at room temperature.

Since the success of Weisenberg (1972) in polymerizing tubulin into microtubules in vitro using a calcium chelator, EGTA (Ethylene-glycol-bis- (-aminoethyl ether) N,N'-tetra-acetic acid), new spindle isolation media have been developed based on the calcium lability of microtubules. Such a medium has been used by Rebhun et al. (1974) for isolation of mitotic apparatuses which can incorporate heterologous tubulin and assemble it into birefringent fibers similar to those of mitotic apparatuses in living cells. A slightly modified version of the isolation medium of Rebhun et al. (1974) was used in this study for most spindle isolation. Glycols are now totally eliminated from isolation media such as these.

Semi-lysed "models" of mitotic cells which preserve some *in vivo* functions and show limited motility have reportedly been obtained by Cande *et al.* (1974). The spindles of such semi-lysed cells are said to lose birefringence when cooled, regain it when warmed, and show some anaphase movement. The mitotic apparatuses isolated by Rebhun *et al.* (1974) will lengthen when heterologous tubulin is added to the medium.

The mitotic apparatus has also been isolated using a dimethyl sulphoxide/glycerol medium (Forer and Zimmerman, 1974), a dithiodipropanol medium (Sakai, 1966), and lithium in seawater followed by storage in cold ethanol and lysis in Triton X-ethanol (Mazia *et al.*, 1972).

None of the isolation methods currently available is entirely satisfactory. Mitotic apparatuses in living cells are cold and pressure labile, whereas mitotic apparatuses isolated in organic solvents have stable birefringence at low temperatures, although those isolated recently by Rebhun *et al.* (1974) are cold labile for a short time after isolation. When isolated in a hexylene glycol medium, mitotic apparatuses contain only about 10% of the dry matter present in the mitotic apparatus *in vivo* (Forer, 1969; Forer and Goldman, 1972), so that much material is lost in the isolation procedure. As mentioned above, chromosome movement like that seen *in vivo* has not been seen in isolated mitotic apparatuses.

Almost all the organisms used for the study of the mitotic apparatus have large numbers of chromosomes, which complicate structural analysis of their spindles, and none of the organisms is well known cytogenetically. These difficulties have been avoided by the use of early embryos of *Drosophila melanogaster* for a structural study

of mitotic spindle formation and function, since D. melanogaster has a small number of well characterized chromosomes (2n=8), and its biology and genetics have long been studied (Sonnenblick, 1950; Lindsley and Grell, 1967). The rapid rate of mitosis (one complete division takes ten minutes or less at this stage) (Rabinowitz, 1941), large size of the embryo (0.2 mm in diameter x 0.5 mm in length), and occurrence of many synchronous nuclei or spindles in a syncytium during early development were also of advantage in this work.

Methods for handling embryos and examining them with light microscopy and TEM are available (Huettner, 1933; Rabinowitz, 1941; Okada and Waddington, 1959; Mahowald, 1963a, 1963b; Fullilove and Jacobson, 1971), and the species offers the eventual possibility of using available mutants with different numbers of chromosomes (Lindsley and Grell, 1967) in order to examine the effects of chromosome content on spindle organization.

Only embryos in the blastema divisions were studied here. Blastema divisions are the tenth through twelfth (or possibly the thirteenth, see Zalokar, 1976) divisions after fertilization. In D. melanogaster the egg is fertilized in the uterus, and at the time of fertilization the first meiotic division of the egg is in progress. Embryos can be deposited immediately after fertilization, or they can be retained in the uterus for a variable period, sometimes until just before the emergence of the larva. The first eight or nine mitotic divisions occur in the interior of the embryo. After the ninth division, nuclei move to the embryo surface, where they remain in a syncytium for three to four more synchronous divisions (Rabinowitz, 1941; Sonnenblick, 1950). After the ninth division pole cells bud off

from the syncytium at the posterior pole of the embryo. These pole cells are readily visible with the light microscope in dechorionated embryos, and they serve as a marker for the beginning of the blastema stage. After a total of twelve or thirteen synchronous mitotic divisions, the embryo surface indents and plasma membranes form, separating the nuclei into individual cells for the first time (Figure 1). After the tenth division, and again after the eleventh division, the plasma membrane furrows inward slightly and reversibly (Mahowald, 1963a), producing a characteristic pebbled surface which can be detected with light microscopy. At the time of the first cytokinesis, as the blastoderm forms, as many as 6500 nuclei (Zalokar, 1976) may be present at the embryo surface, closely packed in hexagonal arrays (Fullilove and Jacobson, 1971). After the blastoderm is formed mitotic synchrony is lost.

Mitosis occurs extremely rapidly in D. melanogaster with one complete division lasting an average of 9.1 minutes in the temperature range of 24°-30° C. At 24° C., the temperature commonly used in these studies, interphase lasts 3.4 minutes, prophase 4.0 minutes, metaphase 0.3 minutes, anaphase 1.0 minute and telophase 0.9 minutes (Rabinowitz, 1941).

When the D. melanogaster egg is laid it is surrounded by an opaque chorion which can be removed with sodium hypochlorite (Hill, 1945) and by an inner vitelline membrane coated with a waxy layer (King, 1970). Both the waxy layer and the vitelline membrane resist attempts at permeabilization (Sonnenblick, 1950). Traditionally embryos have been punctured with a small sharp object to allow penetration of fixative into the embryo, although many agents have been reported to increase perme-

ability of these structures (heptane: Zalokar, 1971; octane: Limbourg and Zalokar, 1973; Triton X-100: Sayles, Procunier and Browder, 1973; ether in 70% alcohol: Widmer and Gehring, 1974; butanol: Fausto-Sterling, Zheutlin and Brown, 1974).

The cytology of the blastema divisions has been well characterized with light microscopy by Huettner (1933) and Rabinowitz (1941) using stained paraffin sections, and the appearance of spindles in the light microscope in this study was compared with the in situ work of these earlier microscopists. Since this stage of development has not previously been studied at the ultrastructural level, it was desirable to investigate the general cytology of the embryo and of spindles in situ. The description of mitosis in situ which will be presented here can be compared with electron microscopic studies of the embryo at later stages, such as the time of blastoderm formation (Mahowald, 1963a, 1963b; Fullilove and Jacobson, 1971) and with work on the ultrastructure of the egg (for review see King, 1970) and spermatocytes (Ito, 1960). The only electron microscopic data on this stage is an occasional micrograph of the cytoplasm of blastema embryos in papers dealing primarily with other developmental stages (Okada and Waddington, 1959; Mahowald, 1963a, 1963b).

It was anticipated that isolation of spindles from the syncytial embryo should be relatively easy since there are no plasma membranes separating nuclei or spindles from each other in the main cytoplasmic mass of the early embryo. Crane fly spermatocyte meiotic spindles had been isolated by Müller (1972), indicating that insect spindle isolation was possible. D. melanogaster mitotic spindles can be isolated using either hexylene glycol (Milsted and Cohen, 1973) or a modified tubulin

polymerizing medium (Milsted, Cohen and Lampen, 1976). Spindles isolated in the latter medium appear under phase contrast to have relatively simple structure, with a small number of major fibers. In the course of this work, it was found that "clean" spindles, free of most adhering cytoplasmic material and remarkably like those described *in situ* by Huettner (1933), Rabinowitz (1941) and Sonnenblick (1950) could be routinely prepared.

Most cells from which spindles have been isolated are eggs or oocytes of marine organisms such as surf clams (Rebhun and Sharpless, 1964; Rebhun *et al.*, 1974) and sea urchins (Mazia *et al.*, 1961; Kane, 1962; Goldman and Rebhun, 1969; Inoué and Sato, 1967; Forer and Zimmerman, 1974). Isolated spindles have also been prepared from some cultured mammalian cells (McIntosh *et al.*, 1975; Sisken *et al.*, 1967), and insect spindles have now been isolated from *D. melanogaster* (this paper) and the crane fly *Pales ferruginea* (Müller, 1972).

Major objectives of this work were (1) the study of the cytology of mitosis in *D. melanogaster in situ* with TEM, (2) the isolation of spindles from this species, (3) the examination of the morphology of whole isolated spindles, ultimately obtaining a three dimensional impression of them, and (4) the visualization with electron microscopy of the spindle fibers seen in light microscopy in order to see if these spindle fibers are composed of microtubules.

The results of this study should further our understanding of mitotic mechanisms, of the structure of the *D. melanogaster* spindle in the blastema stage both *in situ* and after isolation, and perhaps, of the structural basis for the mitotic synchrony seen in this system.

II. Materials and methods

A. Embryo collection

Wild-type *Drosophila melanogaster* were obtained from stocks which had originally come from the Carolina Biological Supply Co., Burlington, N.C. Cultures were maintained on Instant Drosophila Medium (Carolina) supplemented with viable bakers' yeast (Fleischmann's) and kept in half-pint glass bottles stoppered with plastic culture bottle plugs (Carolina). For embryo collection unetherized flies of both sexes were transferred into egg laying chambers consisting of an open ended glass cylinder with one end covered with nylon mesh (32 spaces/inch), through which embryos, but not adult flies, could pass. The other end of the cylinder was covered with a plastic Petri dish cover which had a hole melted in its center in order to facilitate the transfer of flies into the chamber. After transfer the hole was covered with Parafilm (American Can Co., Neenah, Wisc.). A laying chamber was placed in the bottom of a Petri dish which had been nearly filled with 2% agar, the surface of which was covered with a fermented sugar-yeast mixture. Approximately ½ teaspoon sugar and ¼ ounce package of yeast were dissolved in a small amount of warm tap water and allowed to ferment (after Mossige, 1966). The chamber on the agar substratum was placed in a metal pan or glass bowl lined with damp paper towels, all of which was covered in order to exclude light. These chambers were prepared the evening before embryos were to be collected.

Newly fertilized eggs were collected the following morning. Laying chambers were first placed on fresh Petri plates for about 30 minutes, then transferred to another fresh substrate for embryo collection. Fresh food apparently stimulated egg laying. This first thirty minute laying

period of the day allowed flies to lay any eggs which had been fertilized and retained in the uterus. Such eggs were usually advanced in development and were routinely discarded. Embryos for experimental use were collected during a fifteen minute period. With these precautions the majority of eggs collected during the fifteen minute collection period were newly fertilized.

For collection of large numbers of embryos the surface of the agar was washed with a gentle stream of distilled water into a filter apparatus consisting of a plastic Buchner funnel lined with filter paper. Embryos were washed with distilled water or Drosophila Ringer's solution (7.5 g. NaCl, 0.35 g. KCl, 0.21 g. $CaCl_2$ in one liter of water. Ephrussi and Beadle, 1936), then dechorionated with 2.5% sodium hypochlorite (diluted Chlorox) (Hill, 1945) for approximately one minute. Embryos were again washed in Ringer's or water, with a final rinse in distilled water. Gentle suction filtration was used at all steps. The filter paper with the embryos lying on it was removed from the funnel and embryos were transferred into distilled water in glass Petri dishes, where they remained until they reached the blastema stage. Embryo development was monitored using a dissecting microscope with illumination from beneath the specimen. The appearance of the embryo at different stages of development is shown in Figure 1. A newly laid fertilized egg with opaque chorion intact is shown in Figure 1a; a pre-blastema embryo after dechorionation is seen in Figure 1b; the embryo in Figure 1c is at the blastema stage, identifiable because of the typical pebbled appearance of the embryo surface; a blastoderm embryo is shown in Figure 1d for purposes of comparison.

When only a small number of embryos was needed, individual embryos

were lifted off the agar substratum at the end of the laying period with small forceps, and were placed in a depression dish with black electrical tape on its underside, permitting the white embryos to be seen by eye. Washing and dechorionation were carried out in the depression dish, and embryos were later transferred to a glass Petri dish and monitored as described above.

B. Mitosis *in situ*

Embryos of the proper stage were transferred to plastic Petri dishes, to which they adhere, for fixation for transmission electron microscopy (TEM). For manipulating and transferring embryos, small forceps, glass Pasteur pipets and dental reamers (Figure 2) were used. Fixation was usually in Fixative A: 2.5% glutaraldehyde in 0.062 M sodium cacodylate buffer, pH 7.2, with sucrose added to a final concentration of 0.2 M (Fullilove and Jacobson, 1971). Since the vitelline membrane is impermeable to this fixative, a hole was punctured through vitelline and plasma membranes (usually at the posterior pole of the embryo) using a screw-threaded dental reamer (Figure 2). The embryo was punctured within 15 minutes of being covered with fixative and its vitelline membrane was dissected off, after which fixation was allowed to proceed at room temperature for 1 - 2 hours. Fixative B was used in an effort to fix embryos without puncturing them. 10 ml of freshly distilled heptane (a gift of Dr. S. Raps) was shaken with 10 ml of 25% glutaraldehyde for about 5 minutes. Embryos were fixed for 1 - 2 minutes in the glutaraldehyde-containing heptane which had been separated from the aqueous glutaraldehyde phase in a separatory funnel (Zalokar, 1971). After the brief exposure to heptane, embryos were placed in Fixative A (above) in which the vitelline membrane could

Plate I. *D. melanogaster* embryos: tools

Figure 1. *Drosophila melanogaster* living embryos. (a) Embryo with all embryonic membranes. Dorsal chorionic appendages are partly visible (arrows). Chorionic substructure is seen at the posterior pole (arrowhead). (b) Dechorionated embryo, pre-blastema stage. Note homogeneous interior and space between vitelline membrane (VM) and embryo. (c) Dechorionated embryo in the blastema stage. Pole cells (pc) are present, and indentations in the embryo surface can be seen (arrows), which give the embryo surface a characteristic pebbled appearance. (d) Blastoderm embryo, dechorionated. Phase contrast, X 178. Bar is 100 um.

Figure 2. Tools. From top to bottom: screw-threaded dental reamer; straight dental reamer; plastic slide with recessed hole, in which a coated grid is placed; micro-homogenizer pestle of sharpened platinum wire; micro-homogenizer mortar, a 10 µl pipet heated and drawn out to form a constricted region (arrow). X 1.04

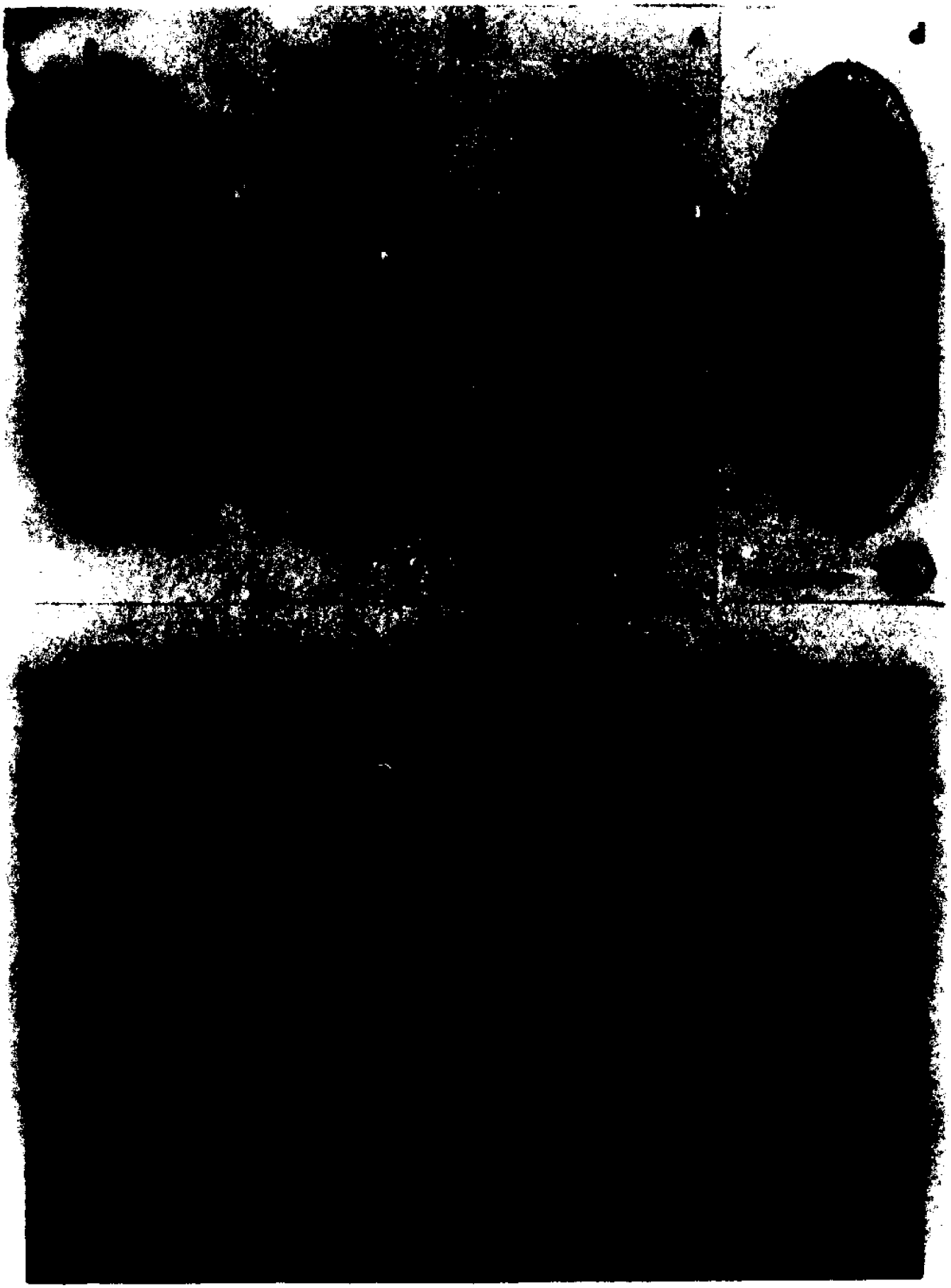

be easily removed without puncturing the plasma membrane of the embryo. Embryos remained in Fixative A for at least another hour.

After fixation in glutaraldehyde all embryos were washed twice for 5 minutes each time in 0.062 M sodium cacodylate, pH 7.2, and were then post-fixed in 2% osmium tetroxide in 0.062 M sodium cacodylate, pH 7.2, for 1 - 5 hours. Embryos were again washed twice in buffer and were often allowed to remain overnight in a third change of buffer. Dehydration was carried out through a standard ethanol series into propylene oxide. Embryos were placed in a propylene oxide-Epon mixture overnight and were flat embedded the next day in fresh Epon mixture in Chang embedding molds (Chang, 1971). The Epon was cured in a 60° C. oven for at least 48 hours. At that time embedments were removed and their rough lower surfaces were recoated with Epon, and embedments were cured another 48 hours. The Epon mixture (R.P. Cargille Laboratories, Inc.) consisted of 26 ml of Epoxy casting Resin D (Epon 812), 17 ml of Epoxy Hardener N.M.A. (Nadic Methyl Anhydride), 12 ml of Epoxy Hardener D.D.S.A. (Dodecenyl Succinic Anhydride) and 0.55 ml of Epoxy Accelerator B B.D.M.A. (N-Benzyl Dimethylamine) (Luft, 1961).

Flat embedments were secured in vise clamp chucks, rough trimmed by hand with single edged razor blades and mounted on a Sorvall MT-2 Porter-Blum ultramicrotome for thick and thin sectioning. Thick sections 0.5 - 2 μm thick were cut with an old Dupont diamond knife for identification of mitotic stage. Embryos were always sectioned perpendicular to their long axis, with the unpunctured pole at the block face. Thick sections were collected with a platinum wire loop and placed on a glass slide, which was then warmed to promote adhesion of the plastic section to the glass. A variety of stains was used on thick

sections. One successful stain was freshly prepared 0.1% toluidine blue in 2.5% sodium carbonate, pH 11 which was applied to the section on a warming tray for about 5 minutes, after which the section could be destained slightly with 70% ethanol if necessary, followed by 100% ethanol, xylene, and immersion oil in which the section was mounted. The other stain which gave satisfactory results routinely was Paragon Multiple Stain for Frozen Sections (Paragon C.N.C. Co. Inc., Bronx, N.Y.), which was applied to the sections for 1 - 2 minutes at room temperature (Spurlock, Skinner and Kattine, 1966). Thick sections were stained in order to visualize chromosomes more easily. Observations of thick sections were made using a Zeiss phase contrast microscope, and sections were photographed with a Nikon camera back mounted on a trinocular microscope head, using Kodak Plus X or occasionally Kodak Tri-X film, developed in Kodak Microdol-X diluted 1:3.

Thin sections for TEM were cut on the same microtome using a Dupont diamond knife, with interference colors of gray - gold, indicating section thickness of approximately 50 - 100 nm. Sections were collected on 200 or 300 mesh copper grids which were sometimes coated with Formvar (0.25-0.3% Formvar 15/95 E Monsanto, Springfield, Mass.) in ethylene dichloride. Staining of thin sections was usually carried out in a Hiraoka Staining Kit (Polysciences). Thin sections were double stained in a saturated aqueous solution of uranyl acetate for 20 minutes (Watson, 1958), followed by 7 minutes in lead citrate (Reynolds, 1963). Best results were achieved when the lead citrate was prepared freshly each time, using newly made 1 N NaOH in boiled deionized, distilled water.

Specimens were viewed in a Hitachi HS-8 electron microscope operated at 50 KV. Micrographs were taken at magnifications between 4,100X and 18,000X on Kodak electron microscope film, estar thick base, which was developed in Kodak D-19 diluted 1:2. TEM negatives were printed on Kodak or Agfa photographic paper, grades 2 - 6 and developed in Kodak Dektol paper developer. Thin sections were examined from 3 interphase, 2 prophase, 1 metaphase and 3 anaphase embryos, and many different spindles in each embryo were observed.

In addition to D. melanogaster embryos, some cells from an established line of D. melanogaster cultured cells were examined for comparative purposes, and as a possible future source of mitotic spindles. The cells were from a line originally established by Schneider (1972) from embryos 20-24 hours old. Dr. R. Sederoff of Columbia Universtiy kindly provided these cells. The cells had been grown in suspension cultures in modified Schneider's medium (Gibco) supplemented with 5% serum. Cultures containing approximately 4×10^6 cells/ml were fixed in 2.5% glutaraldehyde in 0.005 M sodium cacodylate, pH 7, for 2 hours, then were centrifuged and washed twice with 0.062 M sodium cacodylate, pH 7.2. Post-fixation was in 2% OsO_4 in 0.062 M sodium cacodylate, pH 7.2. Subsequent washings, dehydration and embedding were carried out as above, except that some cells were embedded in BEEM hemi-hyperbolic capsules because of small sample size.

C. Isolated mitotic spindles

Spindles were first isolated in Kane's isolation medium (Kane, 1965) consisting of 12% hexylene glycol, 0.01 M potassium phosphate, pH 6.3. Individual embryos in the blastema stage were placed on a slide, and the water drop surrounding the embryo was removed and replaced with a

small drop of isolation medium. When the preparation was covered with a glass coverslip, the weight of the coverslip was usually enough to lyse the embryo. If not, the coverslip was gently tapped. Preparations were examined in Zeiss phase contrast and polarizing microscopes.

For negative staining a small drop of isolation medium containing spindles was placed on a Formvar coated grid and stained with 1% uranyl acetate.

Spindles were also isolated using a modified tubulin polymerizing medium (Rebhun et al., 1974). This medium will be referred to as TPM. It contained 0.1 M PIPES (Piperazine-N-N'-bis-(2-ethane Sulfonic Acid)), 1 mM $MgCl_2$, 5 mM EGTA (Ethyleneglycol-bis-(-aminoethyl ether) N,N'-tetraacetic acid), 10 mM TAME (p-tosyl arginine methylester HCL), and 0.4% Triton X-100, brought to pH 6.8 with KOH. In some preparations 1 mM GTP (guanosine 5' triphosphate) was present.

Preparations intended for phase contrast or polarizing microscopy were made in the same way as those described above. Glass coverslips, rather than plastic ones used for procedures discussed below, permitted the clearest viewing and photography.

For routine preparations the embryos were allowed to develop at room temperature and were lysed into T P M at room temperature (21-22° C.). Additional experiments were performed in which the dechorionated embryos were cooled prior to lysis, in attempts to obtain spindle polar regions in which the microtubule organizing center (M T O C, Pickett-Heaps, 1969) might be seen more easily. Some success was achieved by chilling for approximately 25 minutes at 6° C., followed by lysis in T P M without G T P at room temperature.

For negative staining of spindles for T E M, a mini-homogenizer and

specially designed slide were used (Figure 2). The homogenizer was a 10 µl pipet which had been pulled out so that its inner diameter at the point of constriction was less than the diameter of an embryo. The mini-pestle was a sharpened platinum wire thin enough to pass into the mini-homogenizer. One dechorionated embryo could be drawn up into the homogenizer, along with a small volume of isolation medium (less than 5 µl). When the embryo was punctured with the sharpened wire, the spindles were all contained within the small volume of isolation medium, which could be deposited onto a prepared grid, for example. If desired, part of the homogenate could be placed on a slide for monitoring of mitotic stage of that embryo. The plastic slide had been drilled through, producing a hole smaller than the diameter of a grid, and in addition a second depression had been drilled around the edges of the first hole, producing a recessed platform on which a grid could sit and be viewed with light microscopy. This permitted observation of the fate of the preparation from the time of spindle isolation through negative staining. Grids were sometimes fastened to slides with double stick tape or supported on inverted hyperbolic BEEM capsules to immobilize them during specimen preparation.

Grids were coated with Formvar, with carbon-stabilized collodion (0.5% parlodion in amyl acetate), or with carbon-stabilized Formvar (a gift from the lab of Dr. E. de Harven). Usually these surfaces were treated with polylysine in water (1 mg/ml) (Mazia, Schatten and Sale, 1975), rinsed thoroughly and allowed to air dry before spindles were deposited on the grids. Polylysine coatings promote adhesion of spindles and other negatively charged structures to treated surfaces; this treatment was done in an effort to improve spindle retention in these preparations.

For negative staining, a drop of homogenate was deposited on the grid and allowed to stand for 1 - 10 minutes. As this drop dried up or ran off the grid, 2.5% glutaraldehyde in T P M was added and the preparation was fixed for 1 - 60 minutes. The fix was removed by touching the edge of the grid to filter paper, and a drop of stain was immediately placed on the preparation. Grids were negatively stained for 30 sec. - 1 min., usually in 2% phosphotungstate, pH 7, or in 2 parts P T A at pH 7 to one part 0.1% bovine serum albumin (Dawes, 1971). After staining the grids were again touched to the edge of filter paper, and were then ready for viewing.

For SEM, plastic coverslips were employed (A. H. Thomas Co., Philadelphia, Pa.). These were precleaned for approximately one hour in Micro cleaning solution (International Prod. Corp., Trenton, N. J.), rinsed with water and incubated in a solution of polylysine in water (1 mg/ml, Mazia, et al., 1975) for up to 48 hours, under refrigeration to prevent bacterial contamination. Subsequently, the coverslips were rinsed well in water and allowed to dry. Glass slides were silicone coated (Siliclad, Clay Adams, Inc., N.Y., N.Y.) in order to favor adhesion of spindles to the polylysine-coated coverslips. Embryos in the blastema divisions were lysed between slide and coverslip in TPM without GTP, and the spindles were perfused with additional TPM to remove much of the cytoplasmic debris. Within 5 minutes of lysis T P M containing 2.0 or 2.5% glutaraldehyde at pH 6.8 was perfused under the coverslip, and the preparation, still on the slide, was placed in a moist chamber for 1-1½ hours. The chamber consisted of a Petri dish with moist filter paper in the bottom. Glutaraldehyde was removed by perfusion with several changes of 0.1 M PIPES buffer, pH 6.8. Subse-

quently 1% OsO_4 in 0.1 M PIPES, pH 6.8 was perfused under the coverslip and allowed to remain there for 30-60 minutes, with the preparation again held in the moist chamber. Osmium was then removed by perfusion with several changes of buffer.

Preparations were examined under phase contrast for possible candidate spindles suitable for further SEM processing. In general, the best specimens were those lying alone, free of other spindles and adhering debris. That there were relatively few such spindles remaining is probably due to perfusion, during which spindles were occasionally seen to detach from the coverslip.

The pre-selected coverslip preparations were carefully removed from their slides and placed in small Petri dishes of 0.1 M PIPES, pH 6.8. They were then dehydrated in an ethanol series and passed through a graded series of ethanol-Freon 113 mixtures into 100% Freon 113 (CCl_2 F-CCl_2F). Most of the dehydration, critical point drying, specimen mounting, metal coating and specimen viewing was performed in the laboratory of Dr. E. de Harven at Memorial Sloan-Kettering Cancer Center, N.Y., N.Y. Some samples were also prepared and examined in the laboratory of Dr. T. E. Jensen at Lehman College of The City University of New York, Bronx, N.Y.

Critical point drying (Anderson, 1951) was carried out in Freon 13 ($CClF_3$) (Cohen, Marlow and Garner, 1968) in a critical point dryer designed for processing coverslips (designed by Dr. V. Bystricky, Memorial Sloan-Kettering Cancer Center) or in a Bomar critical point dryer (at Lehman College).

Critical point dried specimens were examined, while dry, under phase contrast. Spindles were still recognizable, and they were

photographed for later reference and their location marked by circling or scratching the region with a Sheaff micro object marker (A. H. Thomas Co.) mounted on the microscope. Appropriate areas of the plastic coverslips were cut out with scissors and mounted on S E M stubs with double-stick tape. Plastic coverslips were used for all S E M preparations because they could be marked and trimmed easily.

Silver conductive paint was applied to the coverslip edges on the stub, and the preparation was coated with approximately 200 Angstroms of gold or gold-palladium in a Denton rotating, tilting vacuum evaporator or in a Hummer sputter-coater. Most specimens were examined and photographed in a Cambridge Stereoscan S4 S E M at 20 KV, using zero tilt for easiest recognition of pre-selected individual spindles when compared with light micrographs (phase contrast). A few preparations were examined in a Jeolco JSM-U3 SEM at 25 KV, 0^{o} tilt. All photographs were taken on Polaroid 55 P/N film, the negatives cleared in sodium sulfite, and prints made on low contrast papers (Kodak F1 - F3). Spindles were observed in 16 different SEM preparations. Usually more than one spindle in each preparation was available for study.

Late anaphase-telophase spindles were examined with T E M after isolation and fixation almost identical to that used for S E M preparations. Many embryos per preparation were lysed between two plastic coverslips, only one of which was treated with polylysine. A grid-work was scratched on the side of the polylysine treated coverslip which was <u>not</u> to have spindles applied to it. This grid-work later simplified location of promising areas of the preparation. Embryos were lysed in T P M without G T P and usually after 5 minutes 2.5% glutaraldehyde in T P M was perfused between the coverslips. All

preparations were placed on a slide in a moist Petri dish and were fixed for at least one hour. Specimens were then rinsed with T P M and post-fixed for 30 minutes in 1% OsO_4 in 0.1 M PIPES, pH approximately 7. After this they were rinsed well with water. At this point the coverslips were separated and subsequent dehydrating solutions were dribbled directly on the coverslip which had been treated with polylysine. Dehydration was through a graded ethanol series into 100% ethanol, then through an ethanol-Epon series directly into 100% Epon. Each step of this dehydrating and embedding took no longer than 5 minutes. Preparations were then examined in order to verify which side of the coverslip had the spindles. Coverslips were cut into conveniently sized pieces with scissors and placed, spindles up in Chang flat embedding molds. More Epon was added to the molds, producing a spindle preparation which was sandwiched between a (sectionable) plastic coverslip and a thin Epon sheet. Specimen blocks were polymerized for 48 hours.

After removal from molds, the preparations were examined under phase contrast and spindles of the desired stage were selected and photographed. These spindles were subsequently relocated for thin sectioning. Often the plastic coverslip was found to peel away from the Epon embedment during trimming. When it did not, its presence made thin sectioning more difficult due to its cutting properties, which differed from those of Epon. Thin sections were collected on Formvar coated slot grids or uncoated mesh grids and stained as described above. It was observed that spindles lay very close to the edge of the Epon embedment, and sometimes the sections tended to curl up along this edge.

III. Results

The term prophase as used here will refer to the mitotic stage between interphase and the appearance of a typical metaphase figure, following the terminology of Huettner (1933). Since spindles of this stage are almost completely surrounded by spindle-delimiting membranes, the term "pro-metaphase" is not directly applicable here.

A. Mitosis in situ

Phase contrast observations

Thick sections (0.5 - 2 μm) of whole embryos embedded in Epon were examined under phase contrast microscopy. Preliminary examination of thick sections permitted the selection of only those mitotic stages desired for further thin sectioning.

Interphase of a blastema stage division is indicated by the presence of nuclei (N) at the embryo surface (Figures 3 and 4). Evidence of the reversible indentations of the plasma membrane which occur after divisions 10 and 11 (Mahowald, 1963a) are seen around many nuclei (arrows, Figure 3). Prophase spindles show a variety of irregular shapes in thin sections (Figure 5). In all cases, chromosomes (ch) can be seen within an enclosing structure, perhaps a membrane. By early anaphasethe boundary between the mitotic apparatus and the cytoplasm, which was very obvious in earlier stages, still remains, although it is not so thick (Figure 6). In favorable spindles (arrows, Figure 6) the boundary is seen as a rather sharp demarcation. Chromosomes are seen to be grouped into sets, and they identify this as an early anaphase section.

Later in anaphase spindles have elongated and chromosome arms are obvious, although relatively few in number (Figures 7 and 8). The sharp demarcation between spindle and cytoplasm seen in earlier stages has

Plate II. Thick Epon cross sections through embryos. Toluidine blue stained. Phase contrast. Bars are 10 μm. In all embryos the vitelline membrane was dissected off at the time of fixation.

Figure 3. Interphase embryo, fixative A. Nuclei (N) and surface indentations (arrows) are seen. X 1647

Figure 4. Interphase embryo, fixative B. Nuclei (N) and many yolk spheres (Y) can be identified. X 514

Figure 5. Near the anterior pole of a prophase embryo. At the pole spindles are present throughout cross sections. Fixative A. Chromosomes (ch) are visible within membrane-bound prophase spindles (arrows outline one such spindle). X 1715

Figure 6. Near the anterior pole of an early anaphase embryo. Spindles (sp) are seen in longitudinal and cross section. Chromosomes (ch) are grouped in sets, and spindles are clearly separated from cytoplasm by a boundary (arrows). Fixative A. X 1715

Figure 7. Anaphase embryo, fixative A. Spindles lie close to the embryo surface and contain chromosomes (ch) in longitudinal section. Yolk spheres (Y) are also visible. X 1260

Figure 8. Anaphase embryo, fixative B. In one of the spindles (sp) seen here, one set of chromosomes (ch) is near the spindle pole. X 1260

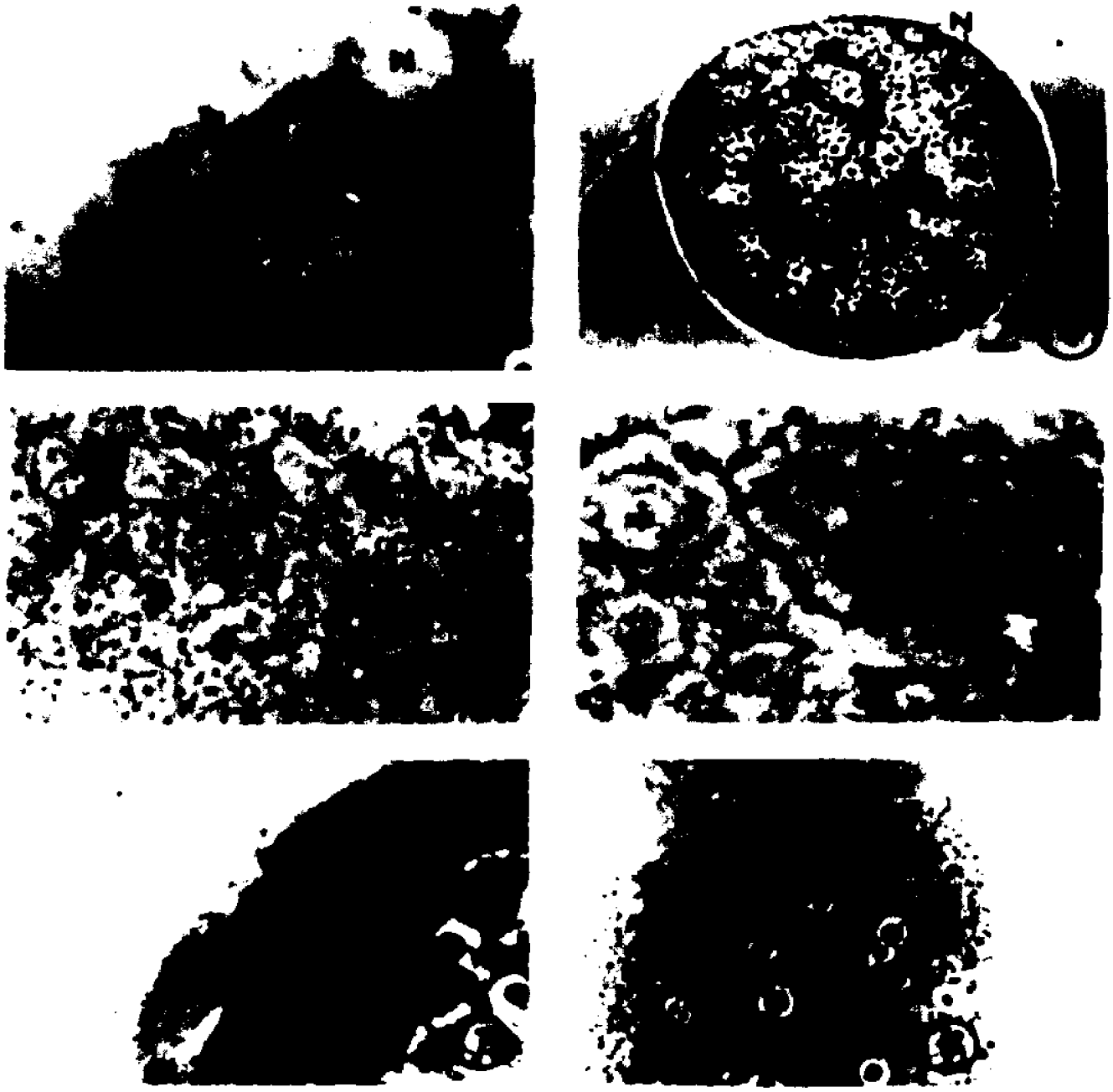

blurred. Spindles appear to lie very close to the embryo surface at this time. In Figure 8 the plane of section passes through one set of chromosomes (ch), and four trailing arms are visible.

TEM

Thin sections were cut from embryos after identification of the mitotic stage. Interphase nuclei (Figures 9 - 11) show circular profiles and are contained by nuclear membranes with ribosomes on their outer surface (arrows, Figure 11). A typical view of a nucleus and surrounding cytoplasm containing mitochondria (m), multivesicular bodies (mvb), extensive rough and smooth endoplasmic reticulum (RER, SER), membrane patches or possible Golgi complexes (*), a dense body (DB) (possibly a lipid droplet or yolk granule), A bodies (A) (King, 1970) and numerous ribosomes is shown in Figure 9.

Gaps in the nuclear membranes are present (arrows, Figure 9), and in cross sections of the membrane no structures corresponding to pore complexes are seen (Figures 9 and 11). In sections tangential to nuclear membranes, however, evidence of pore structure is more obvious (Figure 10). What appear to be remnants of nuclear membrane surface structures, perhaps poorly preserved pore complexes, are seen in some cases (arrows, Figure 10). These measure about 120 - 130 nm in diameter.

Chromatin is generally in a dispersed state, except for a few areas where it may be associated with the nuclear membranes (Figure 9). A small number of cytoplasmic microtubules 24 nm in diameter were seen in this embryo.

In cultured cells of D. melanogaster (originally line 2, Schneider, 1972) pore complexes (PC) are clearly present and the nuclear envelope

Plate III. Interphase embryo. Fixative A. TEM. In these and all micrographs which follow, bars are 1 um unless otherwise stated.

Figure 9. Interphase nucleus (N). The surrounding cytoplasm contains mitochondria (m), A bodies (A), a multivesicular body (mvb), rough endoplasmic reticulum (RER), smooth endoplasmic reticulum (SER), a dense body (DB) and numerous ribosomes. Arrows indicate gaps in the nuclear membranes. X 13,200
**show possible Golgi complexes or areas of SER.

Figure 10. Nuclear membrane of an interphase embryo in tangential section. Chromatin (ch), unidentified 16 nm rings (single arrows) and remnants of pore complexes (double arrows) are seen. X 55,000

Figure 11. Nuclear membranes in cross section, showing ribosomes (r) on the outer membrane. X 50,000


m
m
N
N
10

looks like that classically described (Figures 12 and 13). In Figure 13 continuity can be seen between the outer nuclear envelope and RER. Many cytoplasmic microtubules are seen, sometimes reaching lengths as great as 2 μm. These cells have a prominent nucleolus (Figure 12, Nu); nucleoli are not present in blastema embryos, but appear at the time of blastoderm formation.

Prophase and metaphase spindles are bounded by as many as three sets of membrane layers, each of which is apparently composed of two unit membranes (Figures 14 and 17), separated by a narrow space of variable width. While many discontinuities in these spindle-delimiting membranes are visible with electron microscopy, in thicker sections for light microscopy (Figure 5, for example) there appears to be one membrane surrounding the prophase spindle, from which the impression of an "intranuclear spindle" (Metz, 1926) could arise. These spindle-delimiting membranes do not appear to be typical nuclear envelopes, since there is no suggestion of nuclear pores, nor are ribosomes found on the outer membrane surface alone.

In nearly all thin sections studied from spindles at prophase a membranous area appears in association with the spindle, often, but not always, at what could correspond to a polar region (TM, Figures 14–16). This area may consist of tubular endoplasmic reticulum. Broad expanses of membrane are never seen in any plane of section through such an area, suggesting that these are narrow diameter channels in the cytoplasm. This polar "cap" of membranes is seen to be associated with, and perhaps continuous with, both the membranes surrounding the spindle and the cytoplasmic membrane systems (Figure 16).

Numerous microtubules can be found within the spindle, both in

Plate IV. D. melanogaster cells in culture (Schneider's line 2). TEM

Figure 12. Interphase cell with typical nuclear envelope (NE), pore complexes (PC), nucleolus (Nu), and long cytoplasmic microtubules (mt). X 22,100

Figure 13. Nuclear envelope of an interphase cell in cross section, with pore complexes (PC). The outer membrane of the nuclear envelope is continuous with rough endoplasmic reticulum (arrow). X 49,100

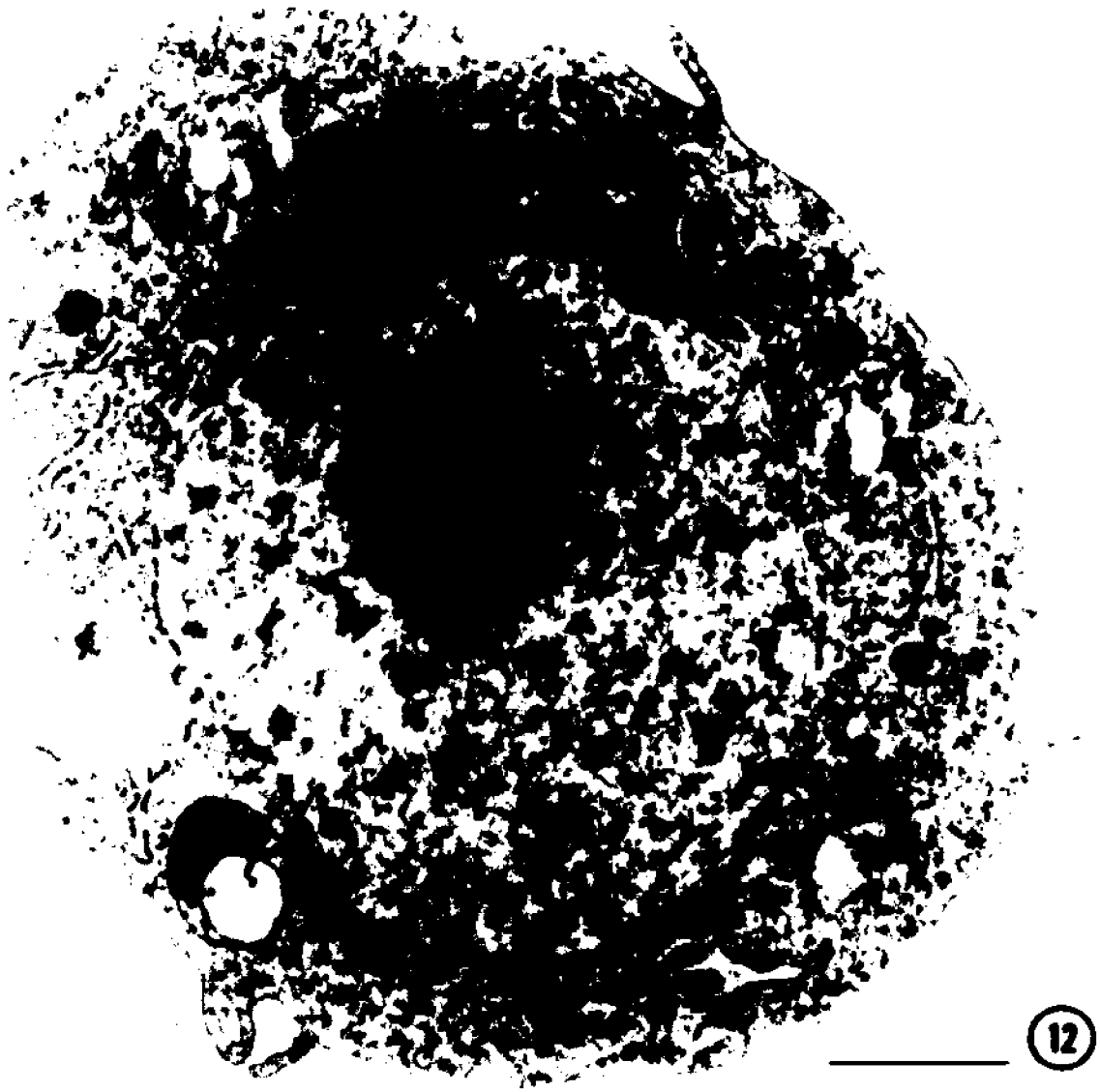
12


PC
D

Plate V. Prophase spindle *in situ*. Fixative A, TEM.

Figure 14. Typical triangular shape of the prophase spindle. A large region of tubular membrane (TM) is obvious. Spindle-delimiting membranes appear to be arranged in two or more layers, each of which is composed of two unit membranes (inset: arrow). Within the spindle chromatin (ch), smooth endoplasmic reticulum (SER), and many microtubules (inset: mt) are present. Mitochondria (m) and an A body (A) are seen in the cytoplasm. X 24,900. Inset, X 34,200


14

Plate VI. Prophase spindle, with adjacent tubular membrane region. Fixative A, TEM.

Figure 15. Prophase spindle, with chromosomes (ch) and an area of tubular membrane (TM) partly visible. X 17,940

Figure 16. Higher magnification view of the tubular membrane region of this spindle Tubular membranes are occasionally seen in circular profile (cp). This "cap" of membranes appears to be continuous with both the spindle-delimiting membranes (single arrows) and cytoplasmic membranes (double arrows) X 27,300

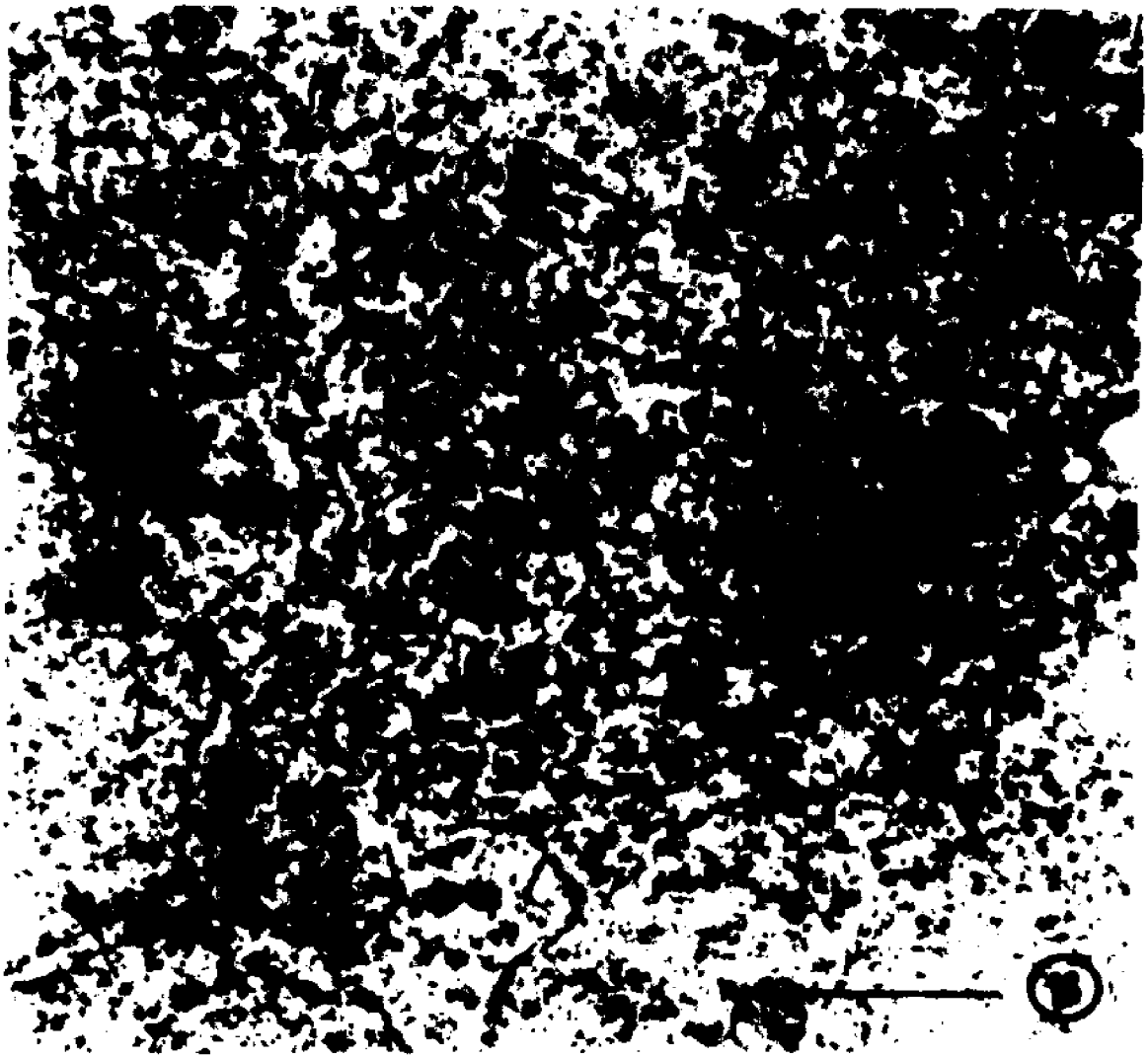

oblique and cross sections (Figures 14 and 17), and condensing chromosomes are visible (ch, Figure 15 and 17). Inside the spindle individual ribosomes can be seen, as well as a small amount of smooth endoplasmic reticulum (SER, Figure 14). Fixation appears to be good, as judged by the appearance of mitochondrial cristae. In thin sections from another prophase embryo a large number of microtubules is present both inside the spindle and immediately outside the first layer of spindle-delimiting membrane (Figure 17).

A probable kinetochore is seen in oblique section in Figure 18 (k) from an early anaphase embryo. In this section microtubules are slightly wavy, and 2 - 3 microtubules are seen to enter the kinetochore directly. Microtubules here have a diameter of about 23 nm.

In early anaphase membranous material around the spindle can still be seen (Figure 19). In most places the membranes appear to be arranged in a double layer with many obvious gaps. At both spindle poles membrane "cap" regions are seen (TM). More SER is also seen inside the spindle, especially towards the poles. Often this SER appears as a circle about 175 nm in maximum diameter. As is the case with prophase spindles, all organelles except individual ribosomes, some SER, microtubules and chromosomes appear to be excluded from the spindle region. "Empty" organelles (L) are probably extracted lipid droplets. Since this Figure is an oblique longitudinal section through an early anaphase spindle, only one set of chromosomes is visible in this section. The spindle lies very near the embryo surface (PM).

In the mid-anaphase embryo examined all organelles appear well preserved (Figures 20-25). Figure 20 is a slightly oblique longitudinal section through an anaphase spindle showing representatives of both

Plate VII. Prophase spindle; kinetochore, Fixative A, TEM.

Figure 17. Spindle-delimiting membranes in a prophase embryo. Within the spindle, chromatin (ch) and many microtubules are present (mt). Immediately outside the innermost membrane layer microtubules are also seen (arrows). X 37,560

Figure 18. Kinetochore from an early anaphase embryo. Microtubules directly enter the kinetochore (k). X 44,100

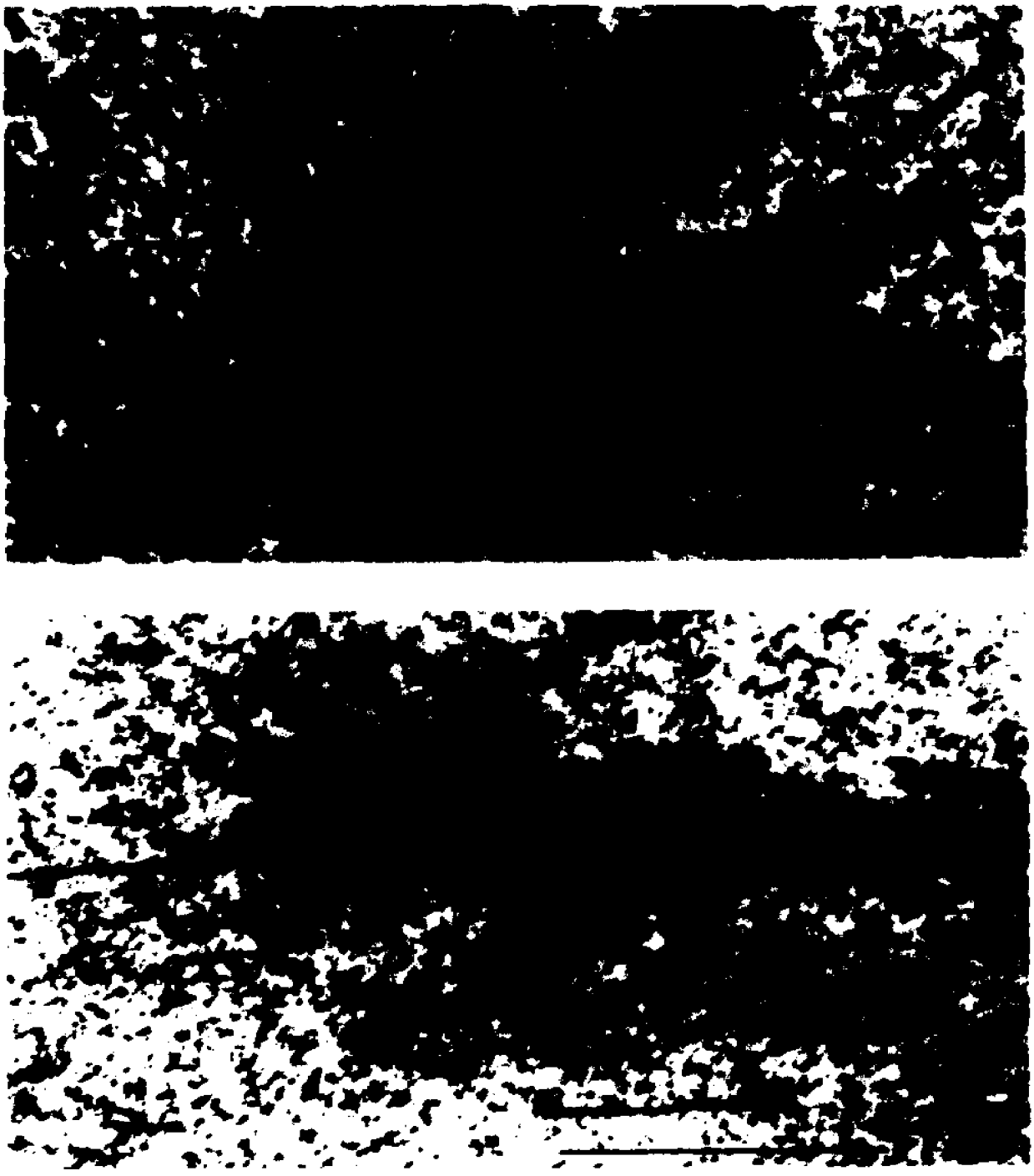

Plate VIII. Early anaphase spindle. Fixative A, TEM.

Figure 19. Slightly oblique section through an early anaphase spindle, showing only one set of chromosomes (ch). Smooth endoplasmic reticulum vesicles are present inside the spindle (arrows), and extensive membranes (TM) are present at both poles. Lipid droplets (L) and the plasma membrane (PM) are also indicated. X 16,900

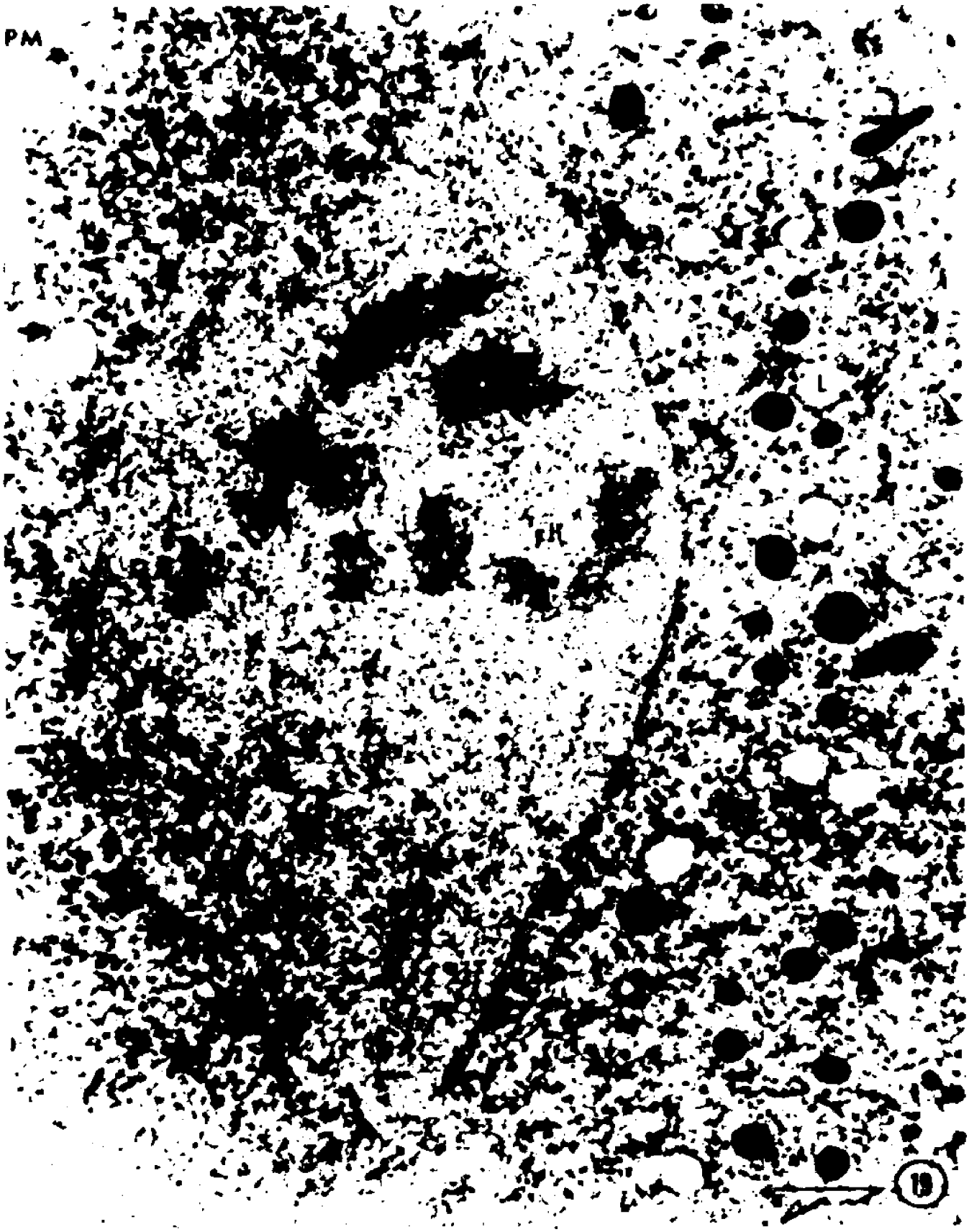
PM
L
FR
19

chromosome sets. Membrane layers still partly surround the spindle, although gaps in the membranes are larger and more frequent in this stage than in earlier stages. Amorphous electron dense material is often seen associated with the spindle-delimiting double membrane layers (arrows, Figures 20 and 21). A tangential section through these membranes at a pole of another spindle in this embryo is also shown (Figure 22). Two main membrane layers are visible, and a suggestion of nuclear pores 120-130 nm in diameter is seen here in the clear circular areas exposed (arrows, Figure 22).

At this stage microtubules are commonly seen both within the spindle, and just outside the membranes surrounding it (Figures 22 and 24). Relatively few microtubules are found outside the spindle, and none have been seen further out into the cytoplasm. Microtubules are not seen in the membrane cap region.

Individual ribosomes are found throughout the spindle, and the circular SER profiles seem to be concentrated at spindle poles. At the pole seen in Figure 23 a large number of such SER vesicles are visible, along with the tubular cap material discussed above (TM). Anaphase spindles would appear to be only partly separated from the cytoplasm by membrane layers, except at their poles, where they are capped by a mass of membranes. The spindle shown in Figure 25, like almost all studied at this stage, lies very close to the plasma membrane of the embryo. Direct continuity of plasma membrane and spindle-delimiting membranes has not been clearly demonstrated, although this micrograph is suggestive of it (arrow). In Figure 20, also, the spindle-delimiting membranes appear to bulge out toward the plasma membrane.

A portion of another anaphase spindle is seen in cross section

Plate IX. Anaphase spindle. Fixative A, TEM.

Figure 20. Longitudinal section through an anaphase spindle, with chromosomes (ch), microtubules (mt) and smooth endoplasmic reticulum (SER). In the cytoplasm a yolk sphere (Y), mitochondria (m) and lipid droplets (L) are found. Arrows indicate electron-dense material associated with spindle-delimiting membranes. X 15,900

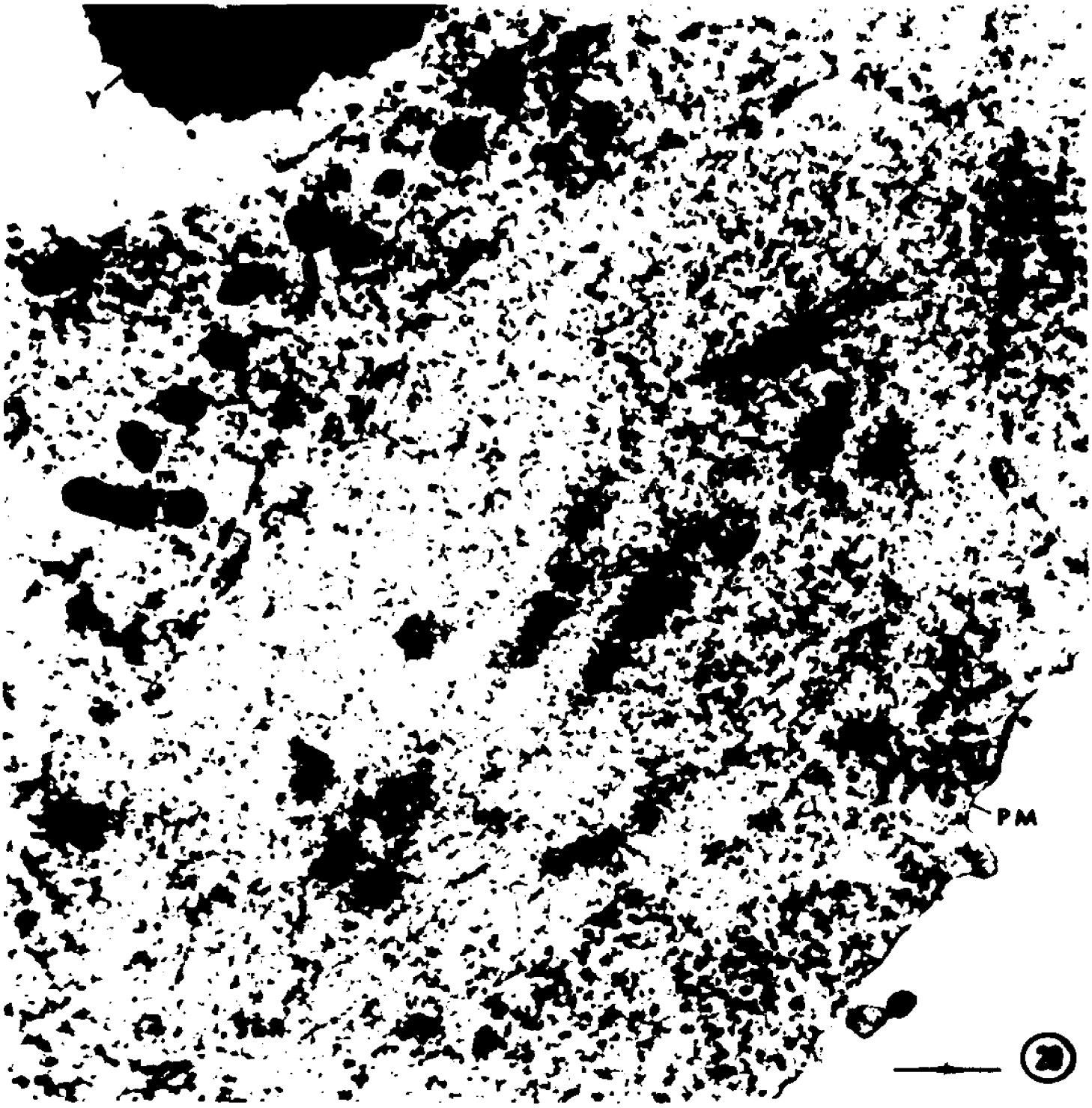
Y
PM
2μ

Plate X. Anaphase spindle-delimiting membranes. Fixative A, T&M.

Figure 21. Cross section through spindle-delimiting membranes in an anaphase embryo. Electron-dense material is associated with layers of membrane (arrow), each layer apparently composed of two unit membranes. Microtubules (mt) are seen within the spindle. X 43,700

Figure 22. Tangential section through the spindle-delimiting membranes of an anaphase spindle. Areas suggestive of pore complexes are indicated (arrows) in the two membrane layers. X 38,500

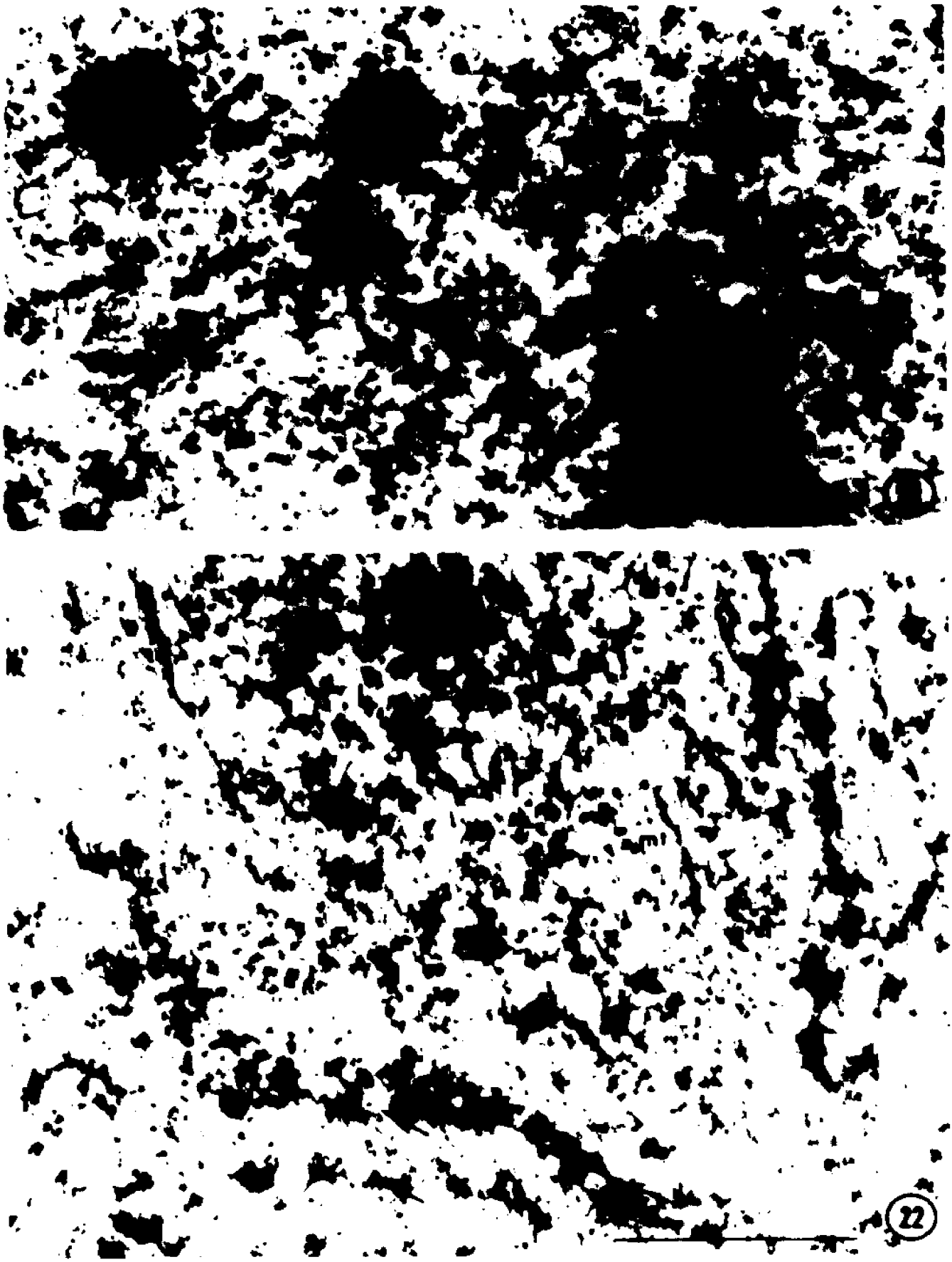

Plate XI. Anaphase spindle pole. Fixative A, TEM.

Figure 23. Extensive membranes at the pole of an anaphase spindle. Areas of tubular membranes (TM) as well as vesicular smooth endoplasmic reticulum (SER) are present. X 28,800

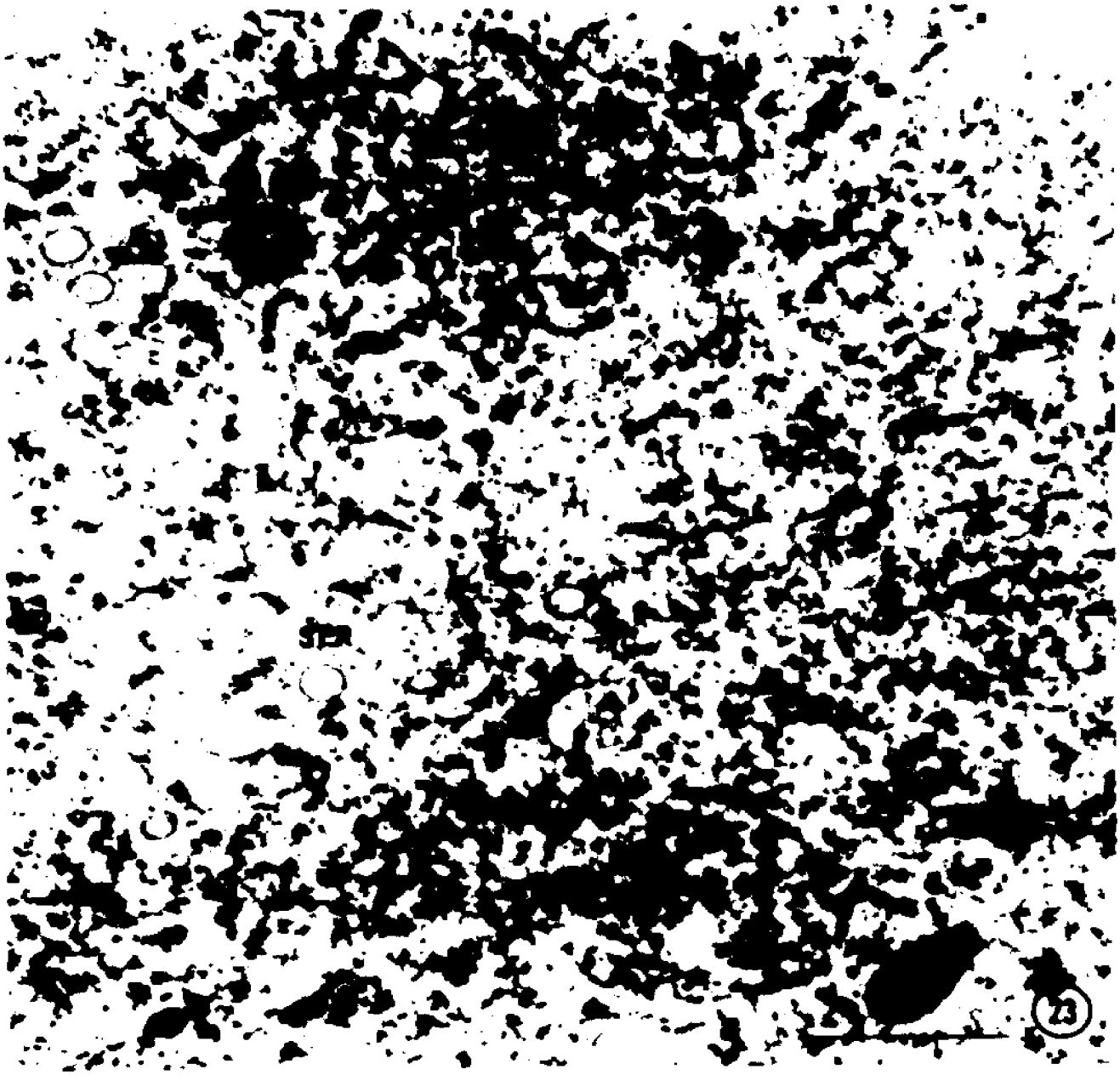

Plate XII. Anaphase spindles and spindle-delimiting membranes. Fixative A, TEM.

Figure 24. Spindle-delimiting membranes in close proximity to cytoplasmic rough endoplasmic reticulum (RER). A microtubule (mt) lies just outside the innermost layer of membranes. Arrows indicate microtubules in a cluster. Such an area might correspond to a spindle fiber. X 37,560

Figure 25. This anaphase spindle lies close to the plasma membrane (PM) and spindle-delimiting membranes appear to lead out in the direction of the plasma membrane (arrow). Inside the spindle chromosomes (ch) and microtubules (mt) can be seen. X 29,000

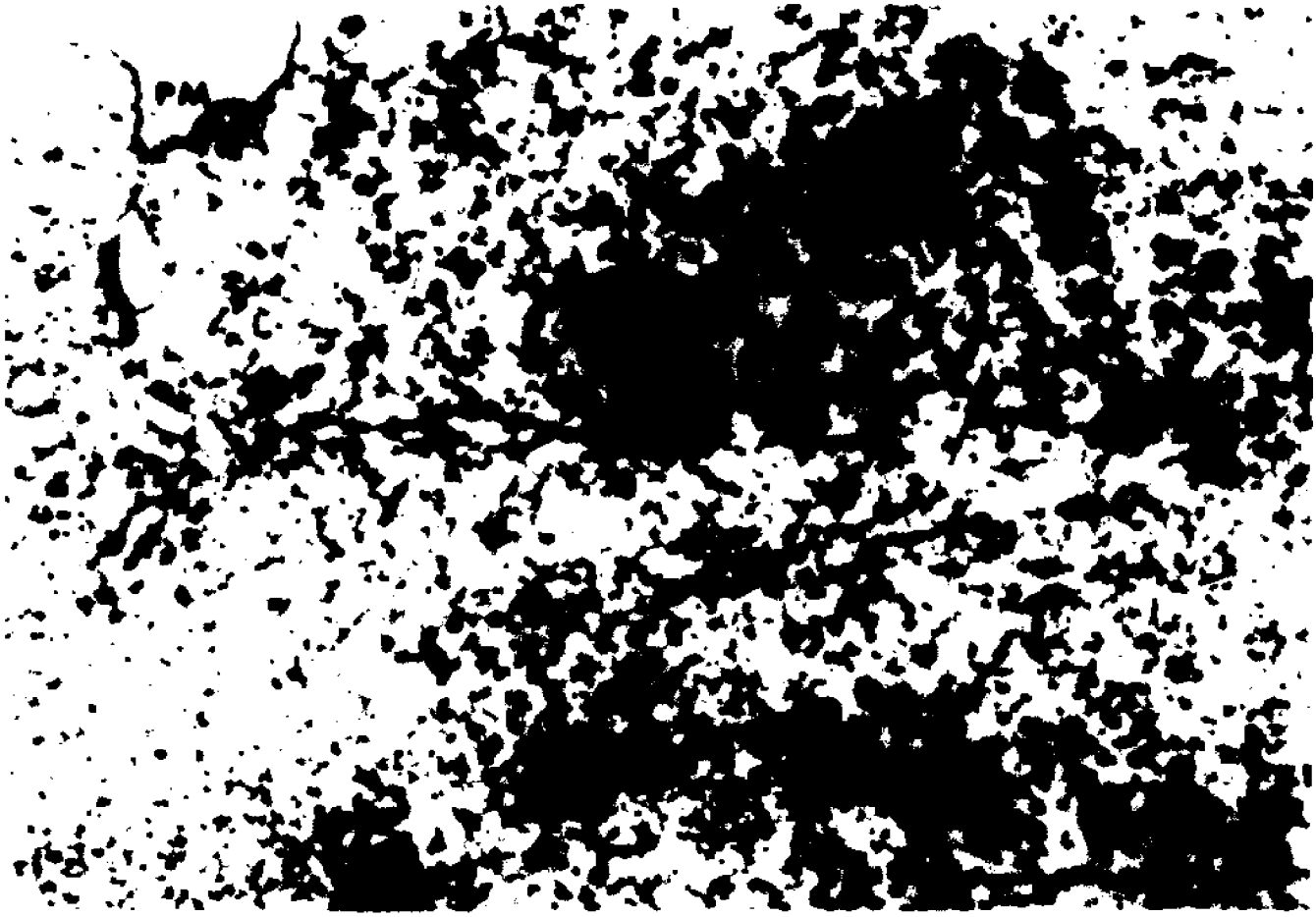

(Figure 24). Many microtubules appear in cross and very slightly oblique sections. Many microtubules appear to be concentrated in one area of the spindle (arrows), perhaps corresponding to a spindle fiber of light microscopy. A lone microtubule is present just outside the spindle-delimiting membranes (mt, Figure 24).

Rough endoplasmic reticulum (RER) is frequently seen near spindle membranes (Figures 20, 21, 24). In some cases the RER appears to lead off into the cytoplasm and might be able to serve as a communications channel between spindles in the syncytium (Figure 24).

Heptane permeabilized embryos

The thick sections of Figures 4 and 8 and the thin sections of Figures 26 and 27 are from embryos pre-fixed with glutaraldehyde in heptane. While fixation appears adequate when viewing thick sections, for electron microscopy consistent fixation was not obtained. In favorable specimens organelles are well preserved (Figure 26; m,L, RER, NE, Y, mt), although nuclei appear "emptier" than with standard fixation methods. In interphase long cytoplasmic microtubules are obvious features (Figure 26).

In the anaphase embryo (Figure 27) the spindle is apparently devoid of all but chromosomes. Spindle-delimiting membranes are still recognizable, although they appear somewhat swollen in comparison with the membranes fixed in Fixative A (Figure 20, for example). In general, organelles close to the embryo surface are not as well preserved as those further in. Even in this example, some organelles appear to be normal (m, Figure 27). Since spindle microtubules are not preserved and fixation is not consistent from embryo to embryo, this method of fixation was not used routinely.

Plate XIII. Interphase embryo. Fixative B, TEM.

Figure 26. Interphase nucleus (N) and cytoplasm in an embryo pre-fixed in glutaraldehyde-containing heptane. A "nuclear envelope" ("NE") can be recognized, and other organelles appear well preserved (RER, Y,L,m). Long cytoplasmic microtubules are obvious (mt). X 27,500

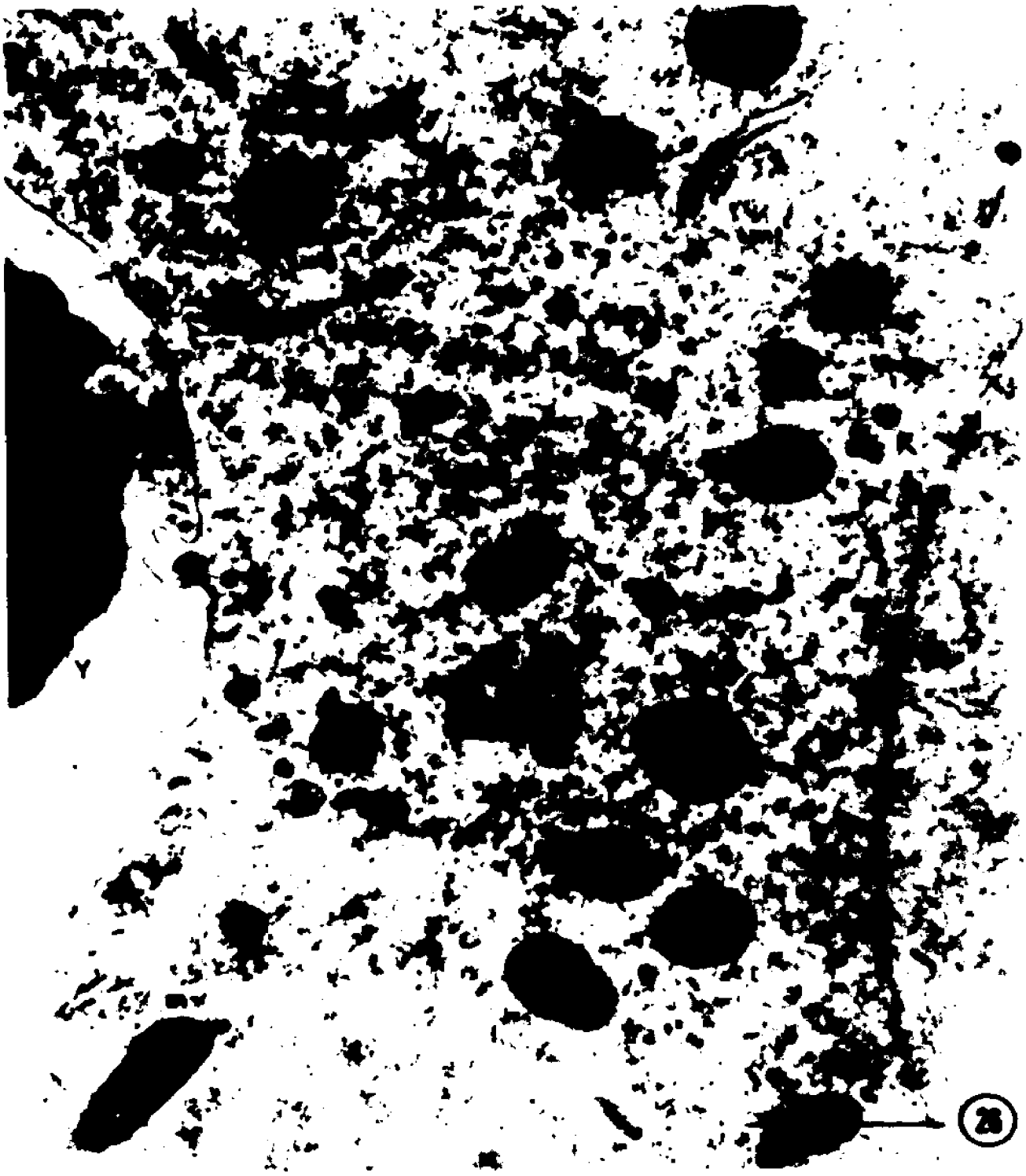
Y
28

Plate XIV. Anaphase spindle. Fixative B, T&M.

Figure 27. Anaphase spindle in an embryo fixed as in Figure 26. The spindle itself appears "empty" except for chromosomes (ch). Membranes in some places several layers thick (arrows) surround the "spindle". X 18,600

B. Isolated mitotic spindles

Light microscopy: Kane's isolation medium

Spindles were first isolated from Drosophila using Kane's isolation medium (Kane, 1965). These spindles were studied with polarized light, under phase contrast, and after staining for transmission electron microscopy.

Embryos will usually burst readily into isolation medium under the weight of a glass coverslip, and most of the contents will spill out of the ruptured vitelline membrane. At low magnifications the spindles are quite difficult to detect in phase contrast, but they are conspicuous in the polarizing microscope because of their birefringence (Figure 28). At higher magnifications in polarized light they appear fibrous, with well defined poles (Figures 29 and 30). At high magnification under phasecontrast spindles which are free of the main cytoplasmic mass are often associated with a surrounding region of non-spindle material which obscures them somewhat (Figure 31). Tapping gently on the coverslip usually removes this adhering cytoplasm, revealing the chromosomes and the fibrous nature of the spindle (Figures 32 and 33). Asters are sometimes apparent (Figure 32), but are not present or are lost in other spindles (Figure 33). In many cases structures measuring about 0.7 μm in diameter appear at spindle poles in the position expected for centrioles (Figure 33). Spindle lengths measure 12 - 15 μm, about the same as for fixed spindles observed in situ by light microscopy (Huettner, 1933).

By means of perfusion experiments under the polarizing microscope some of the stability properties of isolated spindles have been examined. If the isolation medium of fresh spindles is replaced by perfusion with 0.01 maleate, pH 4.5, birefringence remains. However,

Plate XV. Hexylene glycol isolated spindles. Phase contrast and polarization microscopy. The bar in Figure 28 is 100 μm, all others are 10 μm.

Figure 28. At low magnification spindles are seen in polarized light as double bright spots, near and beneath the ruptured vitelline membrane. X 130

Figure 29. Higher magnification view of the area of the rectangle in Figure 28. Spindles (sp) can now be identified as metaphase. X 442

Figure 30. A metaphase spindle trapped under the vitelline membrane (v). Converging fibers and poles are visible. X 1460 polarization microscopy.

Figure 31. Spindles (sp) separated from the bulk of the cytoplasm, partially obscured by adhering cytoplasmic debris. Phase contrast, X 950

Figure 32. Fibrous appearance of an isolated spindle, with chromosomes (ch) visible. Phase contrast, X 1360

Figure 33. Partial asters visible after tapping the coverslip. Chromosomes (ch) and a probable centriole complex (c) are seen here. Phase contrast, X 1140.

Figure 34. A field of anaphase spindles (sp). Separating sets of chromosomes (rather than spindle fibers) render spindles visible. Phase contrast, X 1210.

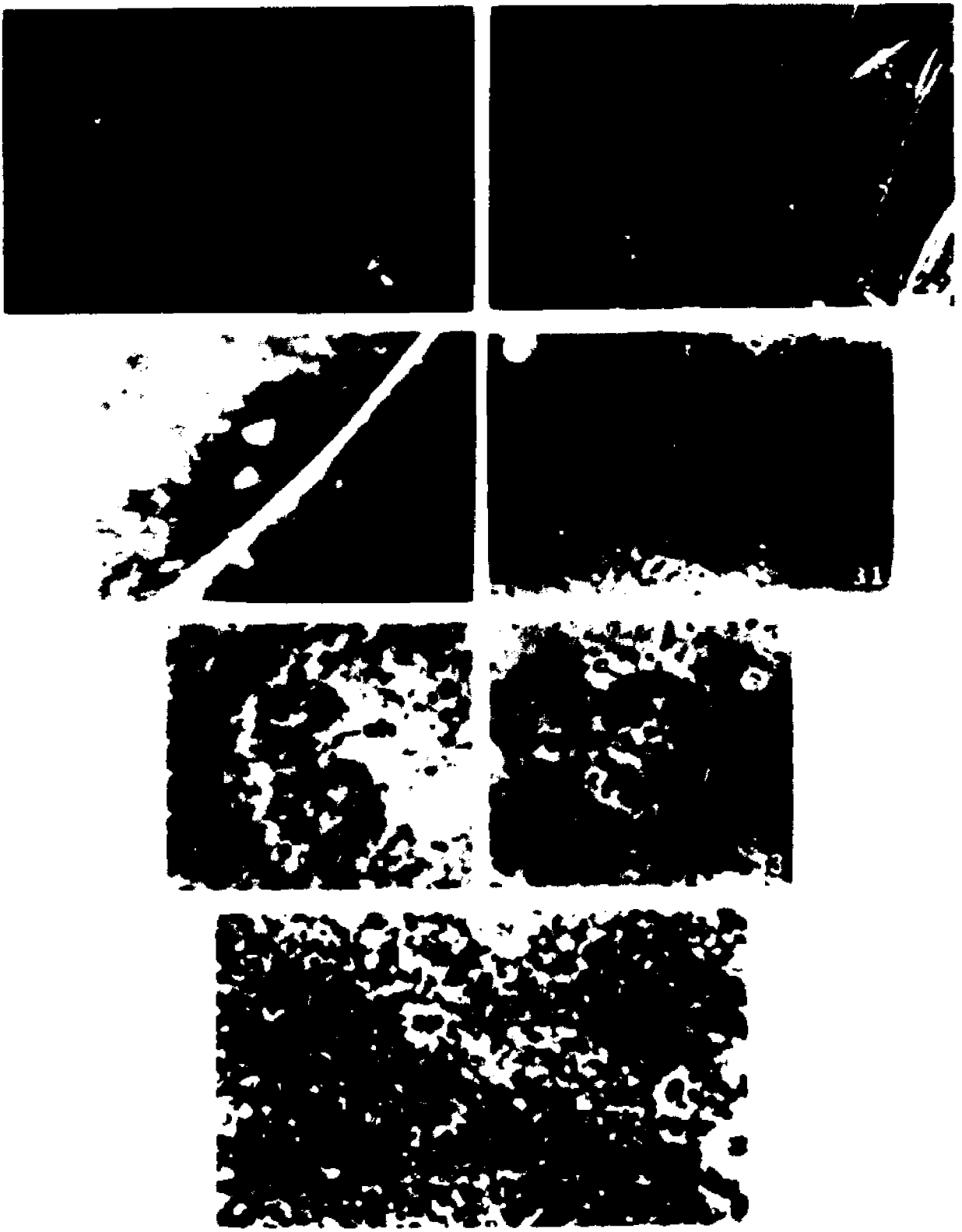

upon subsequent replacement with HCl at pH 2, it disappears rapidly, only partly reappearing upon return to pH 4.5. If freshly isolated spindles are perfused with isolation medium containing a high salt concentration (0.6 M KCl), birefringence quickly disappears.

Storage conditions have also been investigated. When stored in isolation medium at room temperature (about 22° C.) most of the birefringence is lost within 24 hours, and this loss is not prevented by the inclusion of 0.003 M $MgCl_2$ in the storage medium. With 24 hour storage in isolation medium at 0° C., birefringence is retained.

TEM: Kane's isolation medium

When embryos are lysed into Kane's isolation medium and stained with uranyl acetate for TEM examination, isolated bundles of microtubules approximately 20 nm in diameter are found (Figure 35).

Phase contrast microscopy: TPM isolation medium

D. melanogaster spindles isolated by lysis into modified tubulin polymerizing medium (TPM) (Rebhun et al., 1974) are remarkably like spindles of the blastema stage seen in situ (Figure 36 from Huettner, 1933), and their structure appears to better duplicate that of spindles in situ than does the structure of spindles isolated by other methods (for examples, see Figures 31-34). When viewed under phase contrast blastema stage spindles prepared in TPM are easily recognizable even at low magnification and are usually free of adhering cytoplasm. As was noted above for hexylene glycol isolates, all spindles from one embryo are in approximately the same mitotic stage. Occasionally spindles are clumped together in masses, but in most preparations there are many individual spindles which can be examined. Obvious structural features which the isolated spindles share with spindles in situ are spindle

Plate XVI. Microtubules isolated in hexylene glycol isolation medium; major mitotic stages as seen in light microscopy.

Figure 35. Microtubules from an embryo lysed into hexylene glycol isolation medium and stained with uranyl acetate for TEM viewing. Microtubule diameter is 23 nm. X 17,400

Figure 36. From Huettner (1933), Figures 28, 34, 41, 50. Prophase, metaphase, anaphase and telophase spindles, all printed at comparable magnification. From stained paraffin sections of whole embryos.


J5

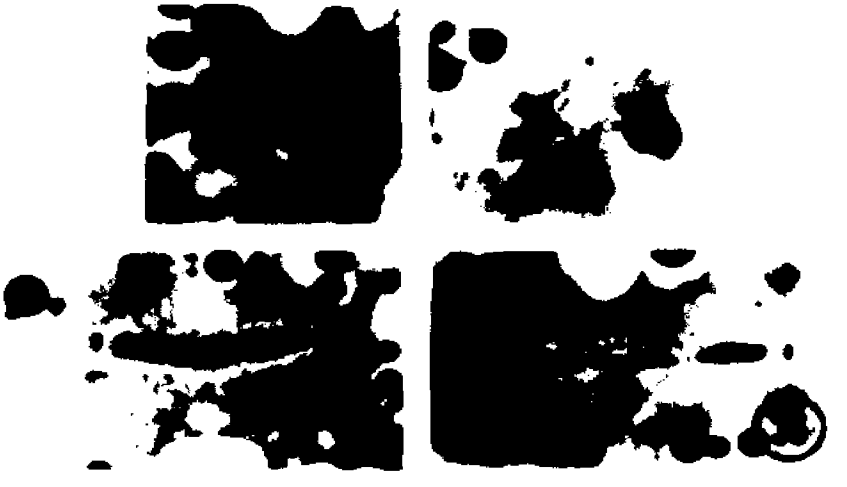

fibers, chromosomes, midbodies and, at the expected locations for centrioles, structures 0.7 μm in diameter. By slight alterations in the timing of embryo lysis all the major mitotic stages can be obtained in different preparations. These are illustrated in Figures 37 - 53 (for representative examples see especially Figures 40, 42, 46, 51).

In a typical field of nuclei from an interphase preparation, the nuclei measure about 8 μm in diameter (Figure 37). Even when nuclei are separated from the main clump of material a boundary of some sort clearly exists around them (arrow). With the presence of 0.4 - 0.5% Triton X-100 in the isolation medium, many membrane components should be disrupted, so that the appearance of "nuclear membranes" in these preparations was somewhat surprising.

Early prophase spindles have two dark structures where centrioles should be found (Figure 38). Since these are too large to be individual centrioles, they will be referred to as centriole complexes as discussed below, indicating that they may represent centriole(s) plus associated material. These centriole complexes are always seen in clean prophase spindles under phase contrast. In Figure 38 a triangular sac-like meshwork of condensing chromatin strands can be seen suspended between the two centriole complexes (arrows).

The prophase spindle in Figure 39 is at slightly later stage than the one in Figure 38. Chromosomes (ch) have begun to appear within the pendulous sac which, with the centriole complexes, comprises the spindle at this stage. The triangular morphology of prophase spindles is most apparent a little later in prophase (Figure 40). Fibrous material can be seen radiating from the centriole complexes (c, c') toward the spindle mid-region. On a line between the two centriole

Plate XVII. Nuclei, and prophase and metaphase spindles isolated in TPM. Phase contrast. The bar in Figure 37 is 100 µm; all others are 10 µm.

Figure 37. A field of nuclei, where even those separated from the cytoplasm seem to be surrounded by a membrane (arrows). X 570.

Figure 38. An early prophase spindle, with two centriole complexes indicated (arrows). Chromatin is visible as the meshwork suspended between the centriole complexes. X 1365.

Figure 39. Somewhat later prophase spindle, with centriole complexes (arrows) and chromosomes evident (ch). X 1015.

Figure 40. A group of prophase spindles. Centriole complexes (c,c'), chromosomes (ch) and chromosome sub-group focal points (arrows) are seen. X 1740.

Figure 41. A prophase spindle trapped in a mass of cytoplasm. The spindle appears to be bound by a membrane (arrows), separating it from the rest of the cytoplasm. Chromosomes (ch) and a centriole complex (c) are also visible. X 1725.

Figure 42. A metaphase spindle. Both centriole complexes (c,c'), chromosomes (ch), a small number of major spindle fibers, and constricted regions at fiber convergence points (arrows) are seen. X 2060.

Figure 43. Two views of a metaphase spindle. Left: small chromosomes (IV) appear to be preceding the rest of the chromosomes towards spindle poles. Right: a centriole complex (arrow) is present a short distance away from the convergence point of the three or four major spindle fibers. X 1015.

Figure 44. Metaphase spindle with some astral material present. Chromosomes (ch) and a constricted region (arrow) between spindle fibers and centriole complex are evident. X 1405.


ch


ch


IV

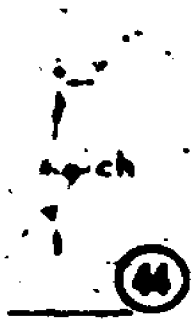
ch

complexes are present two more rather indistinct black areas (arrows). These seem to be focal points for the two chromosome subgroups visible near the spindle mid-region (ch). As in all spindle preparations examined under phase contrast, centriole complexes here measure about 0.7 μm in diameter. These structures are always seen in prophase spindles, usually in metaphase and less frequently in later stages.

The prophase spindle seen surrounded by cytoplasm is clearly defined by a limiting membrane-like structure, giving the impression that the spindle is intranuclear (Figure 41, arrows). Two centriole complexes are present, although only one of them (c) is visible in this plane of focus. The centriole complexes apparently lie outside the spindle-delimiting membrane, and fibers radiating from them towards the chromosomes appear to pass through this membrane. Such a stage was also described by Huettner (1933).

At metaphase spindle poles are well defined by centriole complexes, which sometimes appear square-shaped (Figures 42, 44, 45). A small number of major spindle fibers, usually three or four, are evident between chromosomes and poles. As the fibers converge they coalesce into a constricted "neck" region (arrow, Figures 42 and 44), a short distance from the centriole complex, to which they apparently directly connect. Chromosomes (ch) are seen positioned in the spindle mid-plane. The metaphase spindle of Figure 44 appears to have astral material around both poles. This was rarely seen, and then only in preparations where the isolation medium contained GTP. An unusually clear view of chromosomes is seen on the metaphase spindle in Figure 43 (left). A pair of small chromosomes appears to have moved slightly away from the rest of the chromosomes and advanced a short distance toward the pole. These

Plate XVIII. TPM-isolated anaphase and telophase spindles. Phase contrast. Bars are 10 um.

Figure 45. Flattened early anaphase spindle with many very long fibers (the path of one is indicated with arrows). Chromosomes (ch) and centriole complexes are also apparent here. X 1405.

Figure 46. A late anaphase spindle, with chromosomes massed near poles. Trailing chromosome arms (X), interzonal fibers (if), and four midbodies (mb's) are indicated. X 2060.

Figure 47. Spindles trapped in a mass. Most of them are in late anaphase, such as spindle (A); one is in telophase (T). Presumed centriole complexes (cc) and midbodies (mb) are evident. X 2060.

Figure 48. A very much flattened late anaphase spindle, with four centriole complexes present (cc's) at some distance from the massed chromosomes. X 1725.

Figure 49. A field of telophase spindles on a Formvar-coated grid. Reconstituting daughter nuclei (N) are indicated, and a midbody can be seen in each spindle. X 700.

Figure 50. Telophase spindle with a midbody and a possible centriole complex (arrow). X 700.

Figure 51. A bent telophase spindle, common for this mitotic stage. A single midbody (mb) is present. X 940.

Figure 52. A field of late telophase spindles. Reconstituting daughter nuclei (N) are held together by a short spindle remnant. X 700.

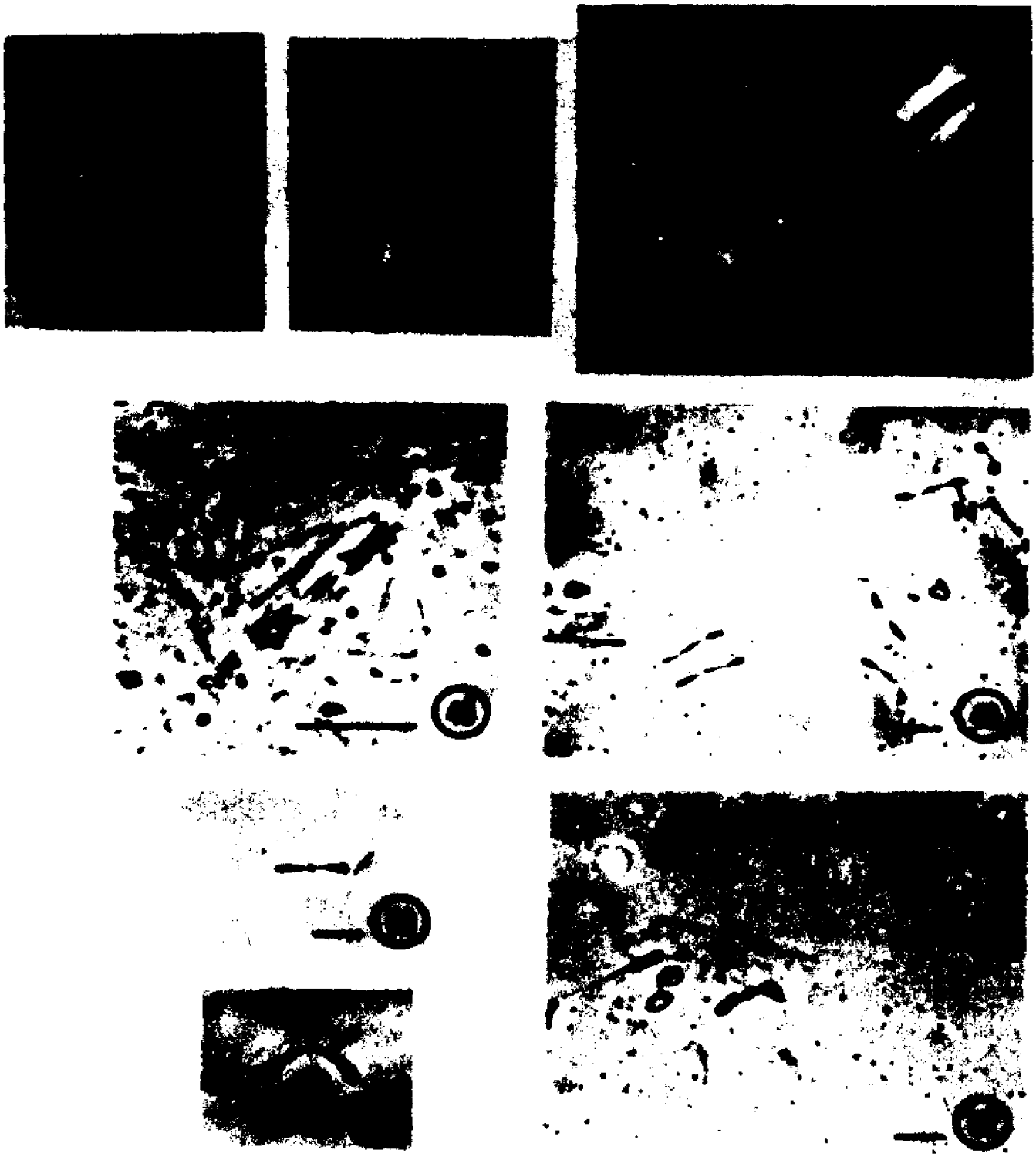

chromosomes are designated as "IV", since Rabinowitz (1941) indicated that the fourth pair of chromosomes precedes the others as they move towards spindle poles.

An early anaphase spindle in which chromosome sets have separated only slightly is shown in Figure 45. Both centriole complexes are visible, and much fibrous material appears in the astral region and elsewhere. Some of the fibrils originating around the lower centriole complex seem to extend well past the spindle midregion into the area otherwise dominated by the upper centriole complex. The path of one such fibril is indicated (arrows, Figure 45). Since GTP was here included in the isolation medium, conditions may have favored polymerization of endogenous tubulin onto spindle astral fibers. This preparation is well flattened onto the coverslip, and even the chromosomes (ch) appear to have flattened and spread.

In all late anaphase spindles a small number of major fibers is present, and each is thickened in the midregion, forming an apparent midbody (Figures 46, 47). In Figure 46, four midbodies are present (mb), and chromosomes are massed at the poles except for a trailing arm in each chromosome set (X). Rabinowitz (1941) identified these arms as belonging to the X chromosomes. In each half-spindle the arms appear to extend towards the same midbody, as if they were associated with the same interzonal fiber. Interzonal fibers (if) visible in Figure 46 are of much smaller diameter than the trailing chromosome arms and appear to be continuous with polar chromatin.

The mass of spindles in Figure 47 includes a telophase (T) as well as anaphase spindles (A), an indication that synchrony in the embryo from which they were isolated is not perfect. Even in such a mass, structural

details such as midbodies and apparent centriole complexes can often be detected with careful focusing.

The late anaphase spindle seen in Figure 48 is very much flattened against the coverslip. As seen in Figure 45, long fibers radiate from the polar regions, sometimes extending past the interzone. Extreme flattening has somewhat obscured details in the interzone but has exposed polar structures. At each pole, some distance away from the polar chromatin, two different sized dark structures are visible. These are in the positions where centrioles should be found; careful differential focusing reveals that these, in contrast to other circular objects seen in the micrograph, are closely adherant to the coverslip and do not appear to be spherical when examined in all planes of focus. In each pair one structure is slightly larger than the other. This would be the image expected if each pair consisted of two roughly cylindrical bodies lying at right angles to each other. Since all four structures are in the size range of 0.5 - 0.9 um, they are all too large to be accounted for by an individual centriole and will be called centriole complexes (cc).

Telophase spindles are seen in Figures 47 and 49 - 53. In Figure 49 spindles of slightly different stages are included. By telophase, spindles have elongated further, and no more than one, relatively large midbody is ever seen (mb, Figures 47, 50, 51, 53). Spindles at this stage seem to be extremely fragile, and very often the entire spindle appears to be curved or bent, as is most obvious in Figure 51. Daughter nuclei have begun to reconstitute at the polar extremities, and a compact interzonal fiber, or possibly a bundle of fibers, separates them (Figure 49). At telophase centriole complexes are seldom seen, although in Figure 50

a possible candidate is indicated (arrow).

By late telophase the reconstituting daughter nuclei (N) are clearly recognizable and are separated by a spindle remnant (Figure 52). This particular stage was very rarely found, although one similar spindle is present in Figure 49. No comparable figures are described in situ by light microscopists (Huettner, 1933; Rabinowitz, 1941).

If embryos are cooled before lysis it is possible to obtain preparations with incomplete spindles and small, sometimes separate polar regions, in which the centriole complex is seen to advantage (Figure 54). A number of points radiate from the dark central structure, the diameter of which is in the range of 0.7 - 0.8 um.

A thread-like structure observed in many preparations is thought to be a sperm tail, due to its wave pattern (Figure 55). This Figure is an example of a preparation in which the embryo contents did not spread well on the coverslip. Consequently, most of the nuclei in the embryo remain trapped in the cytoplasmic mass to the lower right in the micrograph. The sperm tail (arrow) appears to be curved or waved in a regular pattern, sinusoidal in some regions.

Polarization microscopy: TPM isolation medium

Isolated spindles were also checked for birefringence in a few experiments. Spindles were found to be birefringent; Figures 56 and 57 show the same preparation of metaphase spindles in phase contrast (Figure 56) and in polarized light (Figure 57). The late anaphase spindle in Figure 58 also is birefringent. No detailed studies were done with polarized light on this preparation.

TEM of negatively stained TPM isolated spindles

In isolation preparations occasionally an entire spindle was recog-

Plate XIX. Structures isolated in TPM. Phase contrast and polarization microscopy. In Figures 53 and 55 the bars are 100 µm; in all others the bars are 10 um.

Figure 53. A field of telophase spindles in which many spindles are trapped in the cytoplasmic mass (left). In each spindle one midbody (mb) can be seen. X 273.

Figure 54. A spindle polar region from an embryo cooled before lysis into TPM. This structure is the same size (0.7-0.8 um) as the centriole complexes seen at spindle poles. X 1740.

Figure 55. A sperm tail (arrows), a common sight in many TPM preparations. X 273.

Figure 56. Two metaphase spindles and part of a third seen in phase contrast. X 700.

Figure 57. The same spindles as in Figure 56, seen here in polarized light. Chromosomes and birefringent spindle fibers are evident. X 1120.

Figure 58. Anaphase spindle viewed with polarized light. Birefringent spindle fibers are apparent. X 1120.

nizable after negative staining (Figures 59 and 60). In some preparations chromosome-shaped structures about 0.35 μm in diameter were well spread (Figures 60, 61; ch), although more often the whole spindle remained extremely compact and thus was itself not amenable to TEM study. Microtubules were frequently found some distance away from the spindle on the grid.

Figure 62 appears to be a preparation of sperm tail, which is well spread in some areas. (See Figure 55 for a sperm tail in phase contrast). 5 - 9 filaments can be seen spread out in the area indicated by the arrow in Figure 62.

SEM of TPM isolated spindles

Although isolated spindles could be recognized in TEM after negative staining, the whole spindle preparations were too thick to be resolved in the TEM at 50 KV. High voltage TEM might have resolved more spindle fine structure, but another method of examining isolated spindles was more readily available.

The scanning electron microscope has been much used in the study of surfaces of large structures, such as the chorion of the Drosophila embryo shown in Figure 63. Since TPM isolated spindles have already been demonstrated to be clean and, in most cases, free of adhering cytoplasmic debris, scanning electron microscopy (SEM) seemed promising as a new approach to the study of mitotic spindle structure.

The technique which was developed for following the fate of an individual spindle throughout all stages of processing for SEM is illustrated in Figures 64 - 66. In Figure 64 a half spindle is seen under phase contrast, in buffer. Scratches on the plastic coverslip and pieces of debris make convenient markers for spindle location on

Plate XX. Whole spindles isolated in TPM and negatively stained for TEM.

Figure 59. Spindle, on polylysine-coated Formvar, fixed one hour with glutaraldehyde in TPM, stained with phosphotungstic acid in bovine serum albumin. X 7850.

Figure 60. Spindle, with chromosomes (ch) and much fibrous material visible. On polylysine-coated collodion, fixed one minute with glutaraldehyde in TPM, stained with PTA in BSA. X 7850.

Plate XXI. TPM-isolated material after negative staining for TEM.

Figure 61. Well spread chromosomes (ch) and associated material. Chromosomes are about 0.35 um across. This is from the same preparation as Figure 60. X 7830.

Plate XXII. Sperm tail, negatively stained. TEM.

Figure 62. D. melanogaster sperm tail, well spread in many areas (especially at arrow). 5 - 9 filaments are visible. From the same preparation as Figures 60 and 61. X 26,300.

this coverslip. A spindle pole (p) can be seen clearly at one end of the structure, while the other end is less distinct. Trailing fibrous material (arrow) is indicated, as are parallel scratches (double arrows) and bits of debris (d). In Figure 65 the same area of the coverslip is shown after critical point drying. This is photographed under phase contrast, through air. The spindle pole appears as a highly refractile mass (p), and trailing fibrous material is again evident (arrow). Points of reference (d, double arrows) are easily recognizable. In Figure 66 the spindle is shown in SEM. In this and all other SEM descriptions which follow, the term "fibril" will be used to indicate the relatively thin structure seen in SEM, and the term "fiber" will be applied to obvious bundles of fibrils. On the basis of the appearance before critical point drying of this and other spindles on the same coverslip in phase contrast, this preparation was identified as anaphase. A great improvement in resolution, compared with phase contrast, is at once obvious. The spindle pole is seen to be a point of convergence for the many fibrils which make up the half spindle. A three-dimensional impression of spindle structure is especially evident in the pole region (p). The material indicated with the arrow in Figures 64 and 65 is seen in Figure 66 to be a curved fibril. Structures corresponding to chromosomes are not found in any stage of preparation for this particular spindle, suggesting that the spindle was damaged at some time during isolation or fixation rather than during the course of additional SEM preparative steps. Refractile material at the pole in Figure 65 corresponds to the cone-like shape of the spindle pole, where fibrils converge (Figure 66), and density of material is greatest.

Early prophase spindles, as seen with SEM (Figures 68, 69, 70) all

Plate XXIII. D. melanogaster chorion in SEM; example of technique of spindle localization and identification in SEM preparations.

Figure 63. Entire chorion of D. melanogaster embryo, including dorsal chorionic appendages and showing some chorionic substructure at the anterior end. (Compare with Figure 1 for chorionic structure). Bar is 100 um. X 325.

Figure 64. Half spindle, in buffer after fixation and before critical point drying. The spindle pole (p) appears to be a convergence point for light-dense material. Coverslip reference points (d, arrows) are clearly recognizable. Phase contrast, X 750. Bar is 10 um.

Figure 65. Half spindle, seen also in Figures 64 and 66, under phase contrast, after critical point drying. A highly refractile pole (p) is visible, as are bits of debris (d), parallel scratches on the plastic coverslip (double arrows), and a trailing fibril near the spindle (single arrow). X 750. Bar is 10 μm.

Figure 66. Half spindle in SEM. This is the same spindle seen in Figures 64 and 65 and is identifiable by its shape, the trailing fibril (single arrow), and its orientation on the coverslip (not shown in this micrograph). X 2600. Bar is 10 μm.

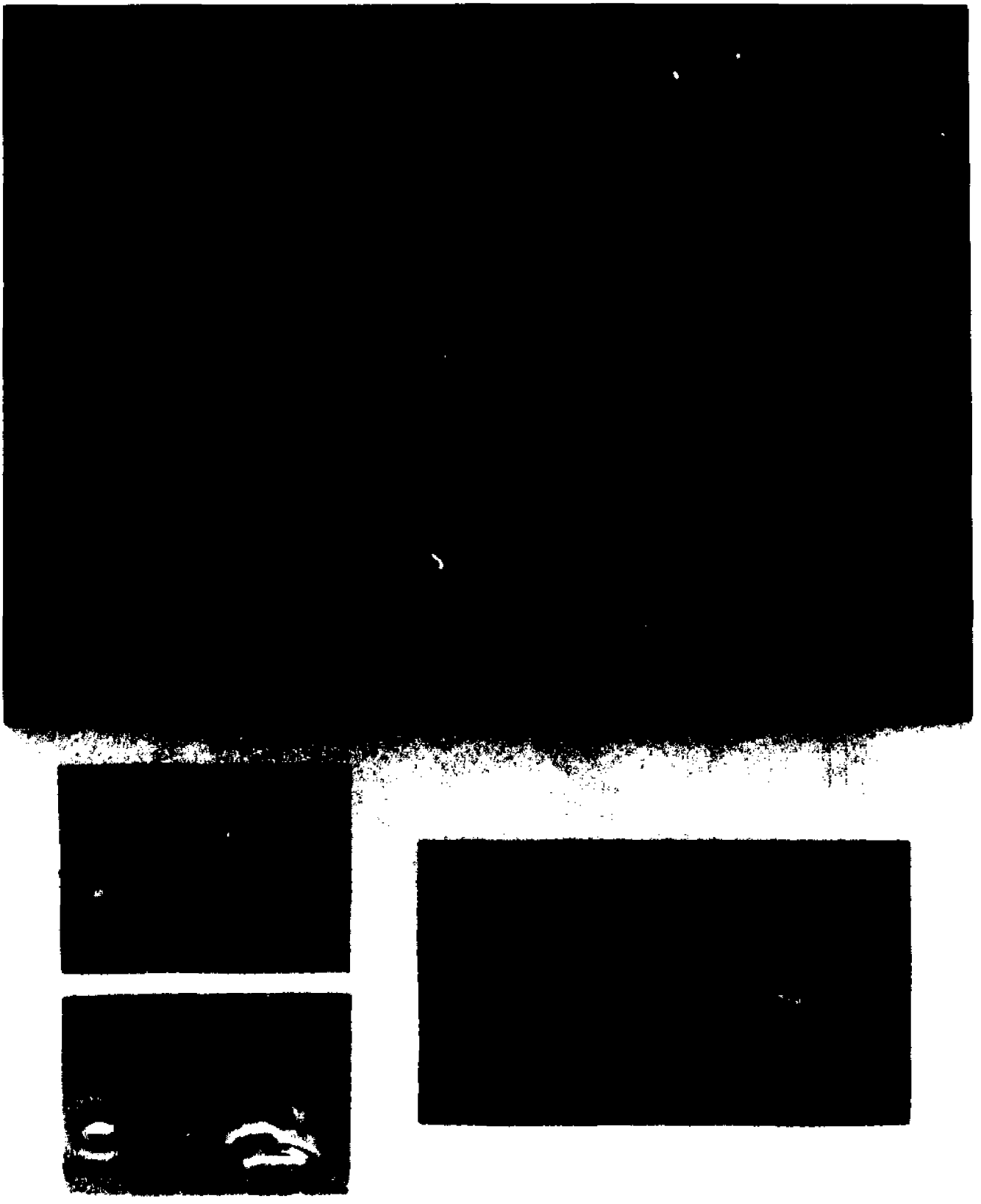

have the appearance of massed, tangled fibrils, often without distinct focal points for the fibrils. In one of the spindles shown in Figure 68, two major focal points are apparent, however (c,c'). As seen in higher magnification in Figure 69 no major fibers are evident, and chromosomes are not visible at this stage using SEM. For comparison, Figure 67 shows the same three spindles of Figure 68 after critical point drying, prior to metal coating. That these are the same spindles is apparent from the corresponding particles and scratches indicated (1, 2, 3). Figure 67 is of course viewed through air, so that much detail is lost, but the light micrograph is valuable in locating good specimens for subsequent scanning, and it suggests the presence of centriole complexes and chromosomes (c,c',ch).

In late prophase spindles such as that in Figure 71, relatively thick, elongate smooth-surfaced structures are found in the position expected for chromosomes on the basis of phase contrast observations of the same preparation. Based upon their thickness range (0.3-0.4 μm) and location these have been identified as chromosomes (ch). At this stage the number of individual fibrils seems rather small, and they are not yet organized into a recognizable spindle with major fibers and distinct poles. Apparent multiple focal points for the fibrils give a criss-crossed pattern to the spindle end-region (arrow).

Metaphase spindles in SEM (not shown here) appear to be thick structures of a classical "spindle" shape, and fibrils are aligned into two cone-shaped half spindles. Little surface detail can be seen, and chromosomes are evidently covered by the surface fibrils.

Spindles in Figures 72 and 73 are from the same late anaphase preparation. In the spindle in Figure 72 any chromosomes present are

Plate XXIV. Prophase spindles in SEM; and SEM compared with light microscopy. All bars are 10 um.

Figure 67. Three early prophase spindles seen under phase contrast after critical point drying. Note landmarks on coverslip (particles 1,2,3). In one spindle apparent centriole complexes (c,c') and chromosomes can be seen, even here where the preparation is viewed through air. X 940.

Figure 68. The same three early prophase spindles shown in Figure 67, in SEM. Particles (1,2,3) and spindle shapes are recognizable, but no evidence of chromosomes is seen, and at the position of the expected centriole complexes (c,c') no polar structures are visible. X 1400.

Figure 69. A higher magnification view of the spindle in Figures 67 and 68 in which presumptive centriole complexes were indicated. Even at this magnification no recognizable structure are seen at those locations. X 7000. SEM

Figure 70. Two prophase spindles, the upper one folded over on itself. As with other prophase spindles, these appear to be masses of fibrils, with no recognizable substructure. SEM, X 2550.

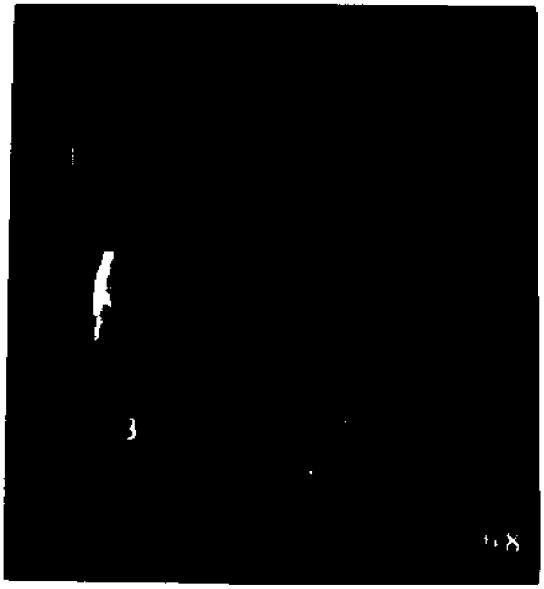

Plate XXV. Prophase and anaphase spindles in SEM.

Figure 71. Late prophase spindle, showing chromosomes (ch) as smooth structures 0.3-0.4 µm in diameter. Towards spindle poles crossed fibrils are seen (arrow). SEM, X 6250.

Figure 72. Late anaphase spindle, somewhat flattened on the coverslip. A small number of fibril bundles are seen in the interzone (if, interzonal fibers). SEM, X 5000.

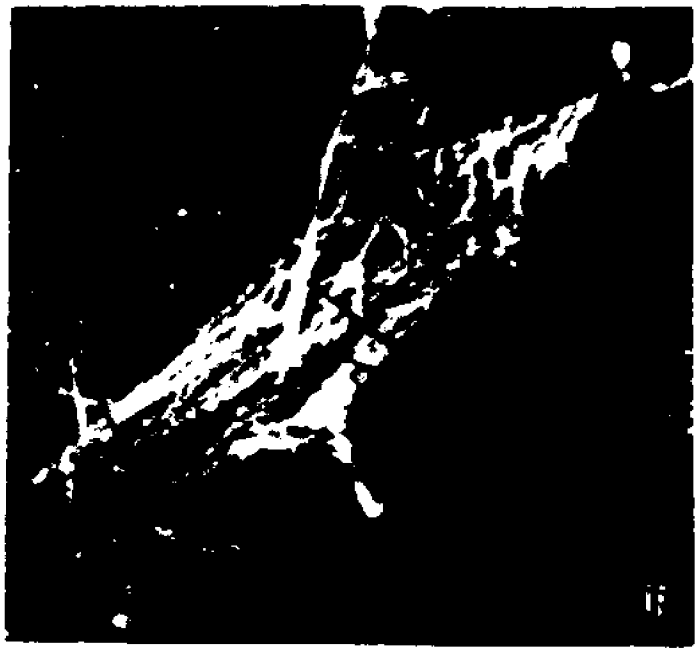

probably buried within the fibril bundles. This particular spindle seems to have flattened against the coverslip, but indications of a small number of major fibers can still be seen in the interzone (if). In the spindle in Figure 73 the poles are well defined by convergence of fibrils, and the midregion of the spindle is composed of a relatively small number of interzonal fibers, each consisting of smaller fibrils. The central fiber (f) is thicker than the others, about 0.7 µm in diameter, with component fibrils in the 0.1 - 0.2 µm range. Apparent astral fibers converge to a series of points at the upper pole (af), while additional astral material seems skewed in the opposite direction at the lower pole.

The lower polar region is seen in greater detail in Figure 74. Chromosomes arms, while buried under fibrils for much of their length, can be seen protruding from the spindle (ch). They are of a different texture and thickness than the fibrils, measuring about 0.4 µm across. A polygonal structure (cc) is present at the position expected for the centriole, adjacent to the fibril convergence point. It appears to have a central body surrounded by a ring of material which itself has regular substructure, with several very thin fibrils leaving the outer edge of the ring at point p. The diameter of the whole structure, including surrounding ring, is approximately 0.7 µm, and its attachment to the rest of the spindle appears rather tenuous. Attached to this structure is a smaller structure about the same size as the inner diameter of the "surrounding ring" described above (arrow). From its position and size the larger polygonal structure has been termed a centriole complex (cc), and the smaller attached body is in the correct position to be a daughter centriole.

Plate XXVI. Anaphase spindles in SEM.

Figure 73. A late anaphase spindle from the same preparation as Figure 72. A small number of interzonal fibers (if) are composed of thinner fibrils, and some astral fibrils (af) are visible at the upper pole. SEM, X 5000. Inset: The same spindle in phase contrast after critical point drying. Highly refractile areas correspond to regions with greatest density. X 940.

Figure 74. Higher magnification view of the lower polar region of the spindle shown in Figure 73. Chromosome arms (ch) are visible, as is a centriole complex (cc), from one point of which (p) three small diameter fibrils diverge. A possible daughter centriole is also indicated (arrow). SEM, X 10,000.

Figure 75. Highly flattened late anaphase spindle, with trailing arms of X chromosomes (X) like those in Figure 46. Bacterial contamination (bc) was present in this preparation. SEM, X 6400.

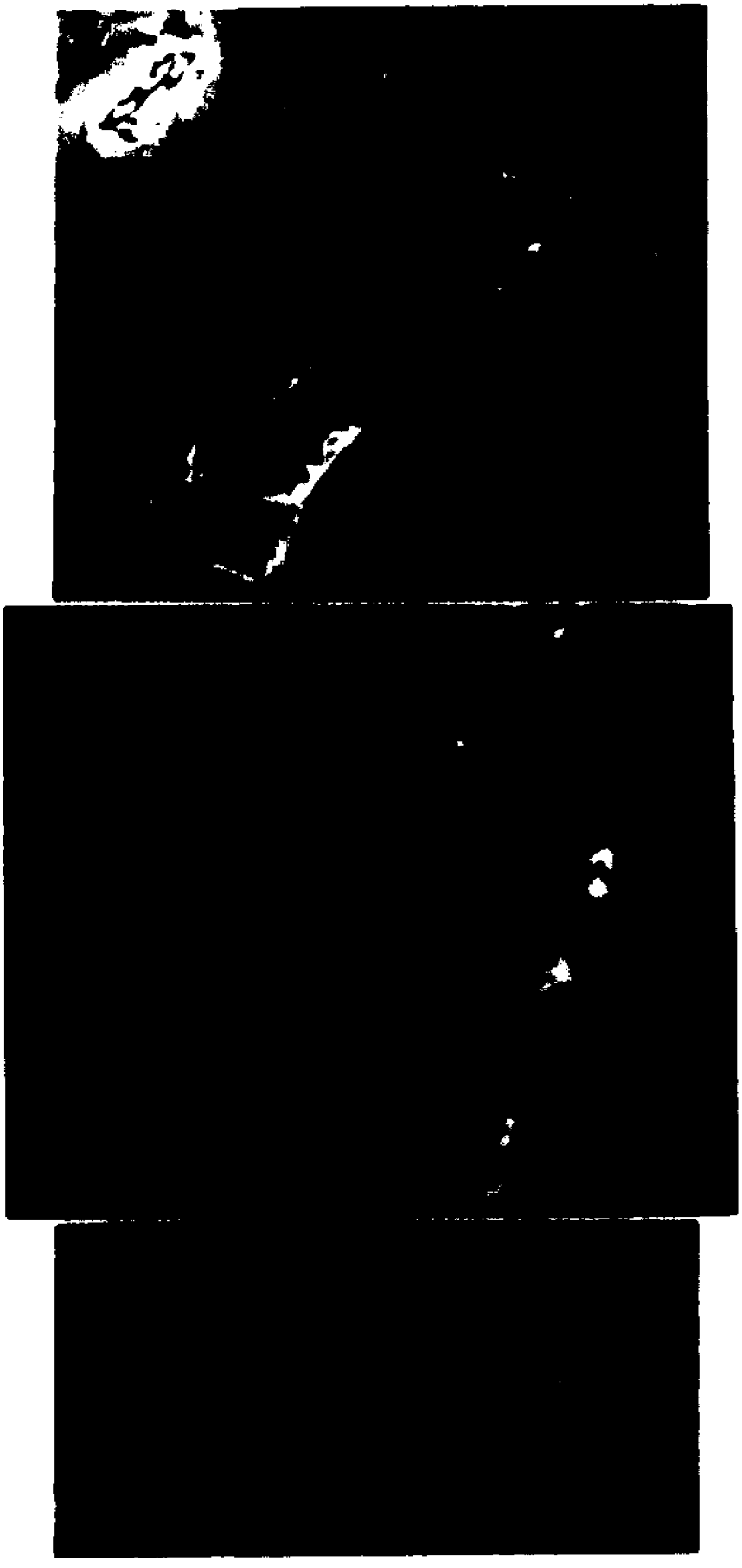

For purposes of comparison this same spindle is shown in the inset in Figure 73 as it appeared under phase contrast after critical point drying, before metal coating. The two highly refractile areas in the inset correspond to polar regions of greatest density in Figure 73.

The very much flattened anaphase spindle in Figure 75, although from a contaminated preparation, demonstrates the trailing X chromosome arms which were described in phase contrast (see Figure 46). The arms (X) are opposite each other on the spindle. These chromosome arms are about 0.3 um wide, and they appear to extend from the polar chromatin mass into the interzone.

In the telophase spindle (Figure 76), reconstituting daughter nuclei (N) are seen at opposite ends of the spindle, which now consists entirely of non-chromosomal fibrils massed together into a compact interzonal bundle about 0.9 um wide at its midregion. This entire spindle is about 16.8 um in length. The whole structure seems twisted, as if one end of the spindle has been rotated with respect to the other. An individual fibril (f) can be seen following a route corresponding to such a twist. On the surface of the daughter nucleus at the left in Figure 76, and seen at higher magnification in Figure 77, there are a number of ring-like features visible (rg), which measure about 0.25 - 0.3 µm in diameter. Structures which might correspond to centriole complexes have not been seen at this stage. The amorphous material adhering to the fibrils in the middle of the interzone might correspond to the midbody which is seen at this stage under phase contrast.

TEM of TPM isolated spindles

Isolated spindles fixed in the same way as the SEM preparations, but dehydrated and embedded in Epon, were thin sectioned in order to

Plate XXVII. Telophase spindle in SEM; TPM-isolated nucleus and telophase spindle in TEM.

Figure 76. Telophase spindle with curved structure. The interzonal fibril bundle seems twisted, as does the path of fibril (f). Reconstituting daughter nuclei (N) are seen at spindle extremities. SEM, X 6250.

Figure 77. Higher magnification view of one of the daughter nuclei in the telophase spindle in Figure 76. Ring-like surface features (rg) are visible here. SEM, X 11,800.

Figure 78. Nucleus (N) isolated in TPM. Chromatin (ch) remains attached to the inner surface of the disrupted nuclear membranes, and some material adheres to outer membrane remnants as well. TEM, X 14,850.

Figure 79. Late anaphase or early telophase spindle with one large midbody (mb) and a trailing chromosome arm (ch). Polar chromatin is condensing into daughter nuclei (N). TEM, X 17,100.

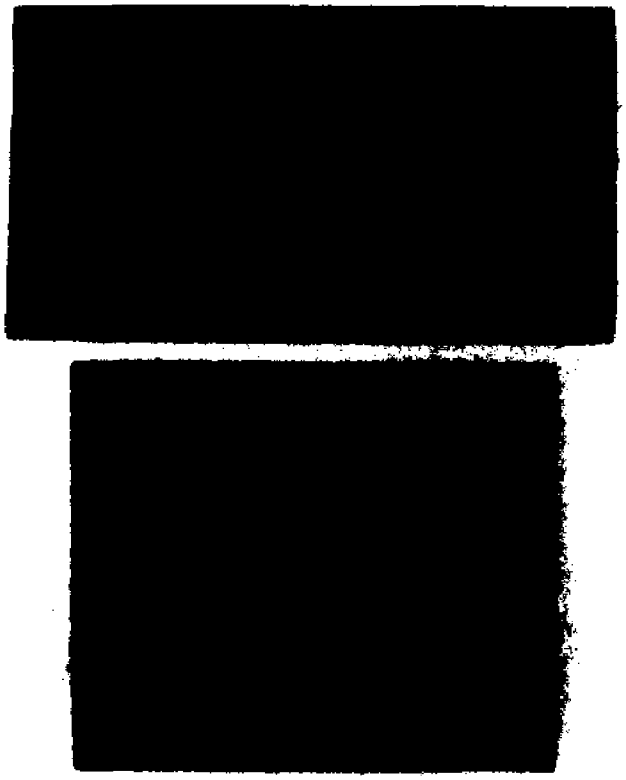

verify the presence or absence of some of the structures which, although clearly present in spindles viewed under phase contrast, were not found using SEM (midbodies, for example). In addition, it was desirable to know how much structural disruption was caused by the detergent (Triton X-100) present in the isolation medium.

A nucleus isolated in TPM is shown in Figure 78. Enough material remains to give the impression of a nuclear boundary, although the material responsible for that appearance seems to be mainly chromatin, attached to remnants of the inner nuclear membrane. Discontinuities in the material do exist, and certainly the inside of the nucleus looks "empty". A few traces of the outer nuclear envelope can be seen, although its absolute identification would be difficult.

A preparation of spindles in late anaphase - early telophase was chosen for more intensive study. Figure 79 shows such a spindle in longitudinal section. A long chromosome arm (ch) trails the rest of the chromatin, which is condensing into a daughter nucleus (N) at the upper pole in this micrograph. A midbody (mb) is seen in the spindle interzone. The electron-dense material which makes up the midbody matrix is clearly different from the appearance of chromatin, when midbody and trailing arm are compared. In Figure 80 the same midbody (from a section at most 8 sections removed from the one shown in Figure 79) is seen at higher magnification. Microtubules appear to enter from both sides of the midbody, indicating that microtubules from the two half spindles might overlap within the midbody. While a regularly repeating pattern is seen in some parts of the midbody material between two microtubules (arrows), distinct crossbridges between adjacent microtubules have not been demonstrated. Ribosomes about 18 nm in

Plate XXVIII. Telophase spindles in TEM.

Figure 80. Late anaphase or early telophase spindle midbody, with microtubules entering from both sides. Some midbody material is arranged in a regularly repeating pattern (arrows). Numerous ribosomes (r) adhere to the microtubules. TEM, X 74,800. Bar is 100 nm.

Figure 81. The same spindle. A grazing section of the midbody or midbodies (mb). A reconstituting nucleus (N) is seen at the upper pole. TEM, X 20,500.

diameter are widely present in these isolated preparations (r), and they line the surface of the polylysine-coated coverslip.

In a grazing section through the interzone of the same spindle, three midbodies and part of a fourth are seen (mb, Figure 81). Such an image could occur if the four anaphase midbodies (Figure 46) had coalesced laterally, forming one larger telophase midbody (see for example Figure 51), which still retains some structural evidence of its origin. The plane of this section has evidently caught the edges of the coalesced midbodies. These (three or four) midbodies are each considerably smaller than the one shown in partial section in Figures 79 and 80.

A cross section through a reconstituting nucleus in a telophase spindle reveals many microtubules (mt) in intimate association with chromatin (Figure 82). Clear zones around the microtubules are not evident here. The presence of these microtubules within the reconstituting nucleus accounts for the SEM image of nuclei at extreme ends of telophase spindles (Figure 76). Apparently the nuclei are held onto spindles by these microtubules, which may function in the movement of nuclei to spindle extremities.

Longitudinal sections through late anaphase spindles are seen in Figures 83 and 84. The chromosomes seen in Figure 84 are surrounded by densely packed microtubules, which would obscure them from view in a SEM micrograph of this stage. Figure 83 is unusual in that it shows a probable kinetochore in an isolated spindle. The kinetochore (k) helps to identify this stage as anaphase, since chromosomal microtubules can be seen between chromosome and pole. Microtubules connect directly to the outer portion of the kinetochore, which is attached to its inner portion by fine fibrous material (arrow). Centriole complexes

were not seen in isolated spindles in TEM.

Plate XXIX. Reconstituting nucleus in a telophase spindle; longitudinal sections from late anaphase spindles.

Figure 82. Cross section through a reconstituting nucleus in telophase spindle. Microtubules (mt) appear embedded in chromatin. TEM, X 68,200.

Figure 83. Kinetochore in a TPM-isolated late anaphase spindle. Fibrous material (arrow) connects the outer portion of the kinetochore with the rest of the chromosome. TEM, X 74,800. Bar is 100 nm.

Figure 84. Chromosome arms (ch) in late anaphase spindle surrounded by many microtubules, closely packed. TEM, X 29,700.

IV. Discussion

A. Mitosis *in situ*

During mitosis in *D. melanogaster* embryos in the blastema divisions, the spindle is surrounded by multiple layers (often 2 or 3) of membranes, each layer apparently being composed of two unit membranes (for example, Figures 14 (inset), 20, 27). "Intranuclear" spindles were described by Metz (1926) in *Drosophila* spermatocytes during prophase and metaphase of meiosis, and later Ito (1960) showed with electron microscopy the presence of 2 - 7 layers of paired unit membranes surrounding the nuclear regions throughout all *meiotic* stages in spermatocytes of *D. virilis*.

Intranuclear spindles are common in many protists and fungi (for a review see Kubai, 1975). In the insects intranuclear microtubules have been described in crane fly spermatocytes (Behnke and Forer, 1966) and in drone honey bee spermatocytes (Hoage and Kessel, 1968).

In *D. melanogaster* embryos the nuclear membranes around interphase nuclei do not look like normal nuclear envelopes. In contrast to typical nuclear envelopes (Figures 12 and 13) these nuclear membranes, shown in Figures 9 - 11, lack obvious pore complexes and show gaps of various sizes. Indeed the possible remnants of pore complexes indicated in Figure 10 look much like the areas suggestive of pore complexes in anaphase spindle-delimiting membranes (Figure 22). The similar appearance, with respect to these areas, of the membranes in interphase and anaphase embryos suggests that perhaps all membranes surrounding nuclei and spindles are closely related to each other and are probably not true nuclear envelopes. Further support for this suggestion is seen in Figures 26 and 27 in embryos fixed in the presence of heptane. Here,

also, (Figure 26) the nuclear membranes do not appear to be typical nuclear envelopes, and membranes around the anaphase spindle (Figure 27) and the interphase nucleus (Figure 26) have a similar morphology.

The presence of layered membranes around the spindle may be related to synchrony of division in this syncytial embryo. Many examples have been reported in which cells which share common cytoplasm or are interconnected by cytoplasmic bridges divide synchronously: D. melanogaster cystocytes (Kinderman and King, 1973), D. virilis spermatocytes (Ito, 1960), drone honey bee spermatocytes (Hoage and Kessel, 1968), rabbit oocytes (Zamboni and Gondos, 1968), and in spermatids of seminiferous tubules (Fawcett, 1961). In many of these cases mitosis is also "intranuclear", so that intracellular contact and the occurrence of intranuclear spindles may be related to each other and to the phenomenon of synchronous division. The situation in the giant amoeba Pelomyxa carolinensis (Roth and Daniels, 1962) is similar to that in D. melanogaster embryos: synchronously dividing nuclei in a syncytium are surrounded by discontinuous membranes (described as remnants of nuclear envelope) throughout mitosis. However, only one set of paired (unit) membranes is visible in the giant amoeba.

Membrane arrangements similar to that shown here for D. melanogaster have been described surrounding the spindles of certain other species. In none of these cases are typical nuclear envelopes present; thus, the term "intranuclear" division is misleading. A general term which could be applied to membranes around spindles in all cases might simply be "spindle-delimiting membranes." This term is broad enough to include all the different forms and arrangements which such memoranes might take

yet clearly describes their location. Ito referred to membranes around Drosophila spermatocyte spindles as "parafusorial lamellae" (1960), but the term "spindle-delimiting membranes" is more general and therefore more widely applicable. The possibility that the spindle-delimiting membranes seen in D. melanogaster embryos are all modified nuclear envelopes cannot be eliminated.

Spindle-delimiting membranes could serve as a partial barrier between the spindle region and the rest of the cytoplasm. Separation of these areas is certainly not complete, since large gaps are present in the membranes, and microtubules are found immediately outside and between layers of the spindle-delimiting membranes (Figures 17, 22, 24). Similarly, microtubules are found outside the spindle during prophase and telophase in crane fly spermatocytes (Behnke and Forer, 1966), suggesting that extra-spindle microtubules may be a feature of insect divisions. Ito (1960) did not see any microtubules in Drosophila spermatocytes after fixation in OsO_4, followed by dehydration in alcohols at about 4° C. It is not likely that microtubules outside the spindle-delimiting membranes are astral microtubules, since they have been seen here in prophase, when asters are not prominent (Huettner, 1933), as well as in anaphase.

A likely function for spindle-delimiting membranes is in control of Ca^{++} level in that region of the cytoplasm. Weisenberg (1972) showed that microtubules can polymerize from tubulin in vitro in the absence of calcium, and that this polymerization is prevented by Ca^{++} concentrations of 6×10^{-6} M or greater. Thus Ca^{++} levels in the spindle region may be critical to the formation of spindle microtubules. The membranes described here may establish areas in the cytoplasm in which different

Ca^{++} levels obtain, thereby establishing conditions for microtubule assembly within the spindle (low Ca^{++} concentration) and preventing polymerization of microtubules outside the region delimited by these membranes (Ca^{++} concentrations greater than 6×10^{-6} M). The membranes may act like the sarcoplasmic reticulum of skeletal muscle, which can accumulate, store and release calcium (Ebashi and Endo, 1968).

A role for calcium ions in spindle and cytoplasmic microtubule assembly in vivo is suggested by the recent work of several different investigators. Kiehart and Inoué (1976) show that Ca^{++} microinjection into dividing echinoderm eggs causes spindle birefringence to disappear from a region approximately equal in size to the injected drop of 1.0 mM $CaCl_2$. The effect is reversible, after which the cell can complete anaphase. Loss of birefringence is seen only when $CaCl_2$ is injected directly on the spindle; concentrations up to 10 mM are ineffective when injected several micrometers away from the spindle, suggesting that the cell must rapidly sequester Ca^{++}. Using the calcium ionophore A 23187 to increase the intracellular level of Ca^{++}, Schliwa (1976) showed reversible retraction and re-extension of Actinosphaerium axopodia. Axopodia shortened when extracellular Ca^{++} concentrations were raised to 0.01 mM or higher. Fuller, Artus and Ellison (1976) describe the depolymerization of the cytoplasmic microtubule complex (CMTC) by increasing intracellular Ca^{++} levels with A 23187, an effect which is also reversible. A role was suggested for Ca^{++} regulation in human granulocyte chemotaxis (Gallin and Rosenthal, 1974). The chemotactic factor C5a (the fifth component of complement) appears to induce intracellular assembly of microtubules during chemotaxis by shifting Ca^{++} out of the cytoplasm in treated cells.

In the Drosophila embryo, in which mitosis occurs very rapidly (about 10 minutes per complete mitotic cycle at this stage in development), it would seem to be of advantage to have any structures involved in regulation of calcium levels in close proximity to the spindle region throughout the mitotic cycle. Spindle-delimiting membranes, and additional membranes discussed below (TM), are in this position. If the membranes are remnants of nuclear envelopes, as suggested by Roth and Daniels (1962) in the giant amoeba, this could be a further adaptation for rapid mitosis in Drosophila, since using nuclear membrane components for a Ca^{++} pumping system would be more efficient than elaborating completely new membrane systems every 10 minutes. If spindle-delimiting membranes do serve in regulation of Ca^{++} levels, the lack of spindle microtubules in the heptane-treated anaphase embryo (Figure 27) might be explained in this way: if heptane rapidly diffused into the embryos, damaging the spindle-delimiting membranes and their Ca^{++} regulatory function (these membranes do look swollen in Figure 27), the immediate effect could be release of Ca^{++} from the spindle-delimiting membranes and rapid depolymerization of spindle microtubules.

Spindle-delimiting membranes appear to be continuous with tubular ER clusters (TM) and with cytoplasmic ER (Figure 16), and, in a few cases, possibly with the plasma membrane (Figure 25). The entire intracellular membrane system may therefore function in a coordinated fashion in the embryo, which seems to be largely specialized for rapid mitosis at this stage of development. This implies communication within the embryo. As first observed by Huettner (1933), when embryos are punctured during fixation, if the puncture is small enough so that no cytoplasm is lost, a gradient of mitotic figures results, with those

closest to the puncture wound being arrested earliest. If, however, the puncture is large and considerable cytoplasm is lost, all spindles in the embryo are fixed at approximately the same mitotic stage. These facts argue against rapid communication systems within the embryo, at least over long distances (approximately 0.5 mm from pole to pole in this embryo). If spindle-delimiting membranes are continuous with the plasma membrane, this may help to explain simultaneous cytokinesis which occurs in Drosophila embryos after the last blastema division (Mahowald, 1963 a). It is unclear how much communication and coordination of events is taking place within the embryo at this time.

Tubular ER (TM, Figures 14-16) is found in obvious clusters at prophase. Such specialized areas of membrane have not been described in blastoderm cells of Drosophila (Mahowald, 1963a, b; Fullilove and Jacobson, 1971) or in Drosophila spermatocytes or oocytes (Okada and Waddington, 1959; Mahowald, 1962; King, 1970), and thus these membrane clusters seem to be characteristic only of the blastema stage of development. Tubular elements of these clusters are of rather constant diameter (30 nm), as is expected for typical tubular SER. SER often functions in transport and metabolism of lipids, and indeed lipid droplets and yolk spheres are common in embryos of this stage. However, another well documented role for SER, in the form of the sarcoplasmic reticulum, is as a pump and reservoir of Ca^{++}, which couples excitation to contraction in the muscle cell (Ebashi and Endo, 1968; see also discussion above of spindle-delimiting membranes). A similar role in the regulation of Ca^{++} levels may thus be performed by SER and spindle-delimiting membranes in this embryo.

SER vesicles clustered at spindle poles are a characteristic

feature of anaphase in the blastema divisions (Figures 18, 20 and 23). Although it is conceivable that they are serving as microtubule initiating sites (MTOC's, Pickett-Heaps, 1969), this is not likely since MTOC's are generally dense, amorphous "fuzzy" regions. Sometimes, however, MTOC's may be associated with membranes, as in the case of some kinetochores and nuclear plaques (Taylor, 1975). In SER-microtubule associations present in early sea urchin embryos the membranes probably function as a Ca^{++} pump (E. Wilk, personal communication). A likely possibility in the Drosophila embryo is that SER vesicles, in addition to the other membranes described above, are active in controlling Ca^{++} levels in the mitotic apparatus.

In early stages of blastoderm formation in D. melanogaster and D. montana, prior to nuclear elongation and cytokinesis, spherical interphase nuclei are closely associated with large numbers of SER tubules and vesicles, which are especially prominent at the future site of cleavage furrow formation (Mahowald, 1963a; Fullilove and Jacobson, 1971). It has been suggested that this might be a major source of material for the newly forming plasma membranes of the individual blastoderm cells (Mahowald, 1963a).

Polar caps, composed of tubular ER and membrane vesicles of greater diameter, are most conspicuous at anaphase. This material, like that discussed above, is in the position expected for microtubule initiation sites and Ca^{++} controlling structures.

In this, the first study of mitosis in the blastema stage, a major objective was the presentation of a general description of mitosis in situ. A thorough examination of serial sections in search of centrioles was not made, and no centrioles were seen. Fullilove and

Jacobson (1971), who made a few scattered observations on pre-blastoderm embryos of D. montana, similarly did not observe centrioles. In the blastema divisions of D. melanogaster it seems most likely that centrioles as described in the blastoderm of D. melanogaster (Mahowald, 1963b) are 160 nm in diameter and only 150-175 nm in length; thus they are shorter than most centrioles and would appear in only 2 - 4 sections at most. As described below, the presence of centriole complexes in isolated spindles of blastema embryos indicates that centrioles and associated material are part of the mitotic apparatus in situ, but were either simply not observed or are not well preserved. In contrast, lower organisms which have intranuclear mitosis usually do not have centrioles (Fulton, 1971), demonstrating that centrioles are not essential for normal mitosis in these organisms, as is also the case in higher plants.

Clusters of ribosomes (presumed polysomes) were seen in the cytoplasm, whereas, inside the spindle, ribosomes usually occurred singly.

Kinetochores seen in oblique section in situ (Figure 18) seem to be sites of microtubule attachment to chromosomes, as expected (Brinkley and Stubblefield, 1970). Microtubules appear to enter the outer portion of the kinetochore at regularly spaced intervals.

In some sections there is an indication of spindle microtubule clustering, possibly forming a structure corresponding to the spindle fiber of light microscopy (Figures 21 and 24). However, even in these areas of increased microtubule density, individual microtubules are still separated from each other, and no connections between neighboring microtubules have been seen. Since serial thin sectioning perpendicular to the spindle axis was not done, the possibility does

exist that inter-microtubule connections do indeed occur here but have not yet been found.

B. Isolated spindles of *D. melanogaster*

1. Properties of spindles isolated in hexylene glycol

Mitotic spindles of individual embryos can be stabilized by lysis into Kane's isolation medium (Kane, 1965). Similar stabilization of crane fly spermatocyte meiotic spindles has been reported by Müller for *Pales ferruginea* (*Nematocera*) (Müller, 1970). *D. melanogaster* spindles exhibit properties consistent with those reported for other species: instability and probable dissolution in high salt concentrations (Kane, 1967) or at low pH (Cohen, 1968), instability of birefringence with storage at room temperature as opposed to 0° C. (Kane and Forer, 1965), and stability at pH 4.5, which is within or close to the isoelectric range (Cohen, 1968).

These spindles can be prepared easily and have the advantage of potential comparison with similarly isolated spindles from other species, since this isolation medium has been extensively used for several years. However, in the case of *Drosophila*, spindles isolated in hexylene glycol appear to contain much more fibrous and non-fibrous material than spindles *in situ* (Figure 36).

Rebhun *et al.* (1975) have shown that the effects of glycols on the *in vivo* mitotic apparatus of surf clam eggs are increases in the volume and birefringence of the mitotic apparatus, in the absence of protein synthesis. Spindles isolated here from *Drosophila* may be showing these same effects of the glycol.

2. Properties of spindles isolated in TPM

Use of an isolation medium based upon tubulin polymerizing condi-

tions and containing protease inhibitor (TAME) and detergent (Triton X-100) as described by Rebhun et al. (1974) allows the preparation of spindles which are not as large and dense as those isolated in hexylene glycol (above). Under phase contrast such spindles are seen to be clean; that is, their structure is readily apparent, as are chromosomes, midbodies and centriolar complexes. This lack of contamination with other cytoplasmic material is probably due not only to selective stabilization of microtubule-containing structures, but also to the dispersive action of detergent on membrane components.

The morphology of spindles after isolation is remarkably faithful to that reported for blastema stage spindles in situ in the older literature (Huettner, 1933; Rabinowitz, 1941). This includes details such as midbodies and trailing chromosome arms in anaphase. Trailing arms were identified as the long arm of the X chromosomes (Figures 46, 76) and "dot" chromosomes (Figure 43) are known to be chromosome IV (Rabinowitz, 1941). Bending of telophase spindles, usually seen in isolates (Figures 49, 51, 53), can also be found in light micrographs of spindles in situ. A major difference between isolated spindles and spindles in situ is noted; polar structures are usually absent in isolated telophase preparations, as judged by observations under phase contrast. According to Huettner (1933) a pair of centrioles is present at each pole in situ at this stage, a relatively long distance away from reconstituting nuclei. This suggests that they are tenuously connected to the telophase spindle and probably fall off during isolation.

The morphology of spindles at various stages seemed the same under phase contrast whether or not GTP was included in the isolation medium.

However, GTP did seem to stimulate formation of background fibrils in the preparation, especially in material from non-mitotic embryos. These fibrils presumably reflect the availability of a polymerizable tubulin pool during interphase.

TPM isolated spindles are birefringent, as expected (Figures 57, 58). While their storage and stability properties were not studied, isolated spindle preparations were examined after negative staining for TEM (Figures 59-61). Microtubules 23 nm in diameter were seen, and occasionally chromosomes were present. Whole spindles generally remain extremely compact and thus are not favorable specimens for negative staining due to their density and thickness.

In order to study spindle structure with the SEM, spindles must be isolated and free of debris, and they must retain the in situ morphology which is characteristic of different mitotic stages. These criteria are met by TPM preparations.

3. SEM analysis of spindle structure

SEM improves upon both the resolution and depth of field obtainable with light microscopy, providing a three-dimensional view of the entire spindle. Comparable spindle reconstructions from serial thin sections and TEM are difficult to achieve and require excessive amounts of labor by comparison. For examination of general structural organization of isolates, SEM might also serve as an alternative to high voltage transmission electron microscopy (McIntosh et al., 1975).

With respect to small sample preparation methods for SEM, use of polylysine-coated coverslips (Mazia et al., 1975) permits the following of individual spindles under phase contrast through all of the processing steps. They can be photographed after critical point drying (Fig-

ures 64, 67) for subsequent identification in the SEM using spindle orientation and adjacent "landmarks" (Figures 64-68). Polylysine-coated plastic coverslips have proven more convenient for marking and cutting than either polylysine or Formvar-coated glass coverslips (Lung, 1974). However, significant losses of material have been encountered; better retention of material might be achieved by covalent linking to the substratum (Vial and Porter, 1975).

At the present time this is the only study of spindle structure in which the SEM is utilized; thus comparison with the data of others is not yet possible and therefore problems of identification of some structures may arise. For interpretation of SEM data, light microscopy and TEM of isolated spindle preparations have proven most useful.

Based on these results it seems likely that SEM will become an increasingly powerful tool for such work as improvements are made in the areas of instrument resolving power, specimen retention, and reduction or elimination of the metal specimen coating.

4. Phase contrast versus SEM

In general, there is good agreement between phase contrast and SEM observations in terms of spindle size and shape, indicating that spindle morphology is little altered during SEM preparative steps. In phase contrast much of the spindle is effectively transparent, so that structures such as chromosomes and centriole complexes are readily visible. Comparison of phase contrast and SEM micrographs (Figures 40 and 68, for example) shows that this is not the case for SEM, as anticipated; in prophase spindles the chromosomes are hidden beneath a fibrous surface. At later mitotic stages smooth-surfaced oblong structures appear, thicker than the surrounding fibrils, which are identified as

chromosomes. In the late anaphase spindle in Figure 73 some of these are visible, and it is likely that others are concealed within the fibrous polar regions. The best evidence that these structures are chromosomes is their location in flattened spindles such as shown in Figure 75, in which two trailing arms of X chromosomes are seen.

The major fibers seen in metaphase and anaphase spindles under phase contrast (Figures 42, 43, 46, 47) are found to be bundles of smaller fibrils in the SEM. Many of these fibrils are in the range of 0.1 - 0.2 μm thick, a size which could accommodate about 6 - 25 microtubules. (This estimate takes into consideration the thickness of the metal coating, but ignores possible clear zones or intermicrotubule material). In some cases fibrils observed in the SEM are thin enough to be accounted for by single metal-coated microtubules (for example, fibril "f" and the fibrils radiating from point "p" in Figure 74). The apparently single interzonal fiber observed in telophase spindles under phase contrast (Figures 49-51) is similarly found to be constructed of smaller fibrils (Figure 76).

The structures seen at spindle poles under phase contrast and referred to as centriole complexes (Figures 38-45, 47, 48, 50) have a maximum dimension of approximately 0.7 μm, and the central black body of polar regions isolated from cooled embryos is about the same size (Figure 54). This value seems too great to be accounted for by a simple centriole or centriole pair, even if measurement error is considered. Mahowald (1963b) reported that the centrioles of D. melanogaster in the blastoderm stages have a maximum diameter of 0.175 μm and are not been found in fully formed pairs. Fullilove and Jacobson (1971) and Fritz-Niggli and Suda (1972) show centrioles surrounded by satellites in the

forming blastoderm of D. montana and in spermatocytes of D. melanogaster, respectively. The diameter of these complexes is in the range of 0.6 - 0.8 μm, which correlates well with the size of the structures seen at poles under phase contrast.

In the polar position of some spindles, SEM reveals a structure of roughly polygonal shape, about 0.7 um in diameter, with a central body approximately 0.2 μm in diameter (Figure 74). This object could be a complex of centriole plus accessory material, possibly satellites, which would serve as the polar microtubule organizing center for these spindles (Pickett-Heaps, 1969). While satellites have rarely been reported surrounding mitotic centrioles (de Harven, 1968), their presence has been shown around meiotic centrioles of D. melanogaster (Fritz-Niggli and Suda, 1972) and in the jellyfish Phialidium gregarium (Szollosi, 1964).

One structure seen easily in phase contrast and not yet identified in the SEM is the midbody (Figures 46, 47, 50, 51, 53). While its absence could indicate loss of some midbody material during SEM preparative steps, a different explanation may hold: the midbody, as seen in phase contrast, could simply be a region of increased density due to overlap of interzonal microtubules of opposite polarity and/or intermicrotubule material (Paweletz, 1967; McIntosh et al., 1975). Such differences in internal density would not be expected to appear under SEM.

An interesting feature of telophase spindles is the substructure at the surface of reconstituting nuclei seen in the SEM (Figure 77). These appear to be coils of rings of material about 0.25 - 0.3 um in diameter. In an SEM study of isolated mouse liver nuclei, Kirschner, Rusli and Martin (1975) found that nuclear pore complexes are resistant to treatment with Triton X-100. However, the features described

here are several times larger than typical pore complexes. It is possible that they are exposed chromatin coils, but further work is obviously needed using a higher resolution SEM on isolated telophase and interphase nuclei in order to clarify the nature of these features.

5. TEM observations

These TEM observations were made in order to verify the presence or absence of structures which are visible with light microscopy, for example midbodies, yet are not apparent in SEM. Such studies were therefore limited to a few selected cases.

Interphase nuclei were examined for the effects of Triton X-100 on nuclear envelopes (Figure 78). A few remnants of outer or inner membrane persist, ind'cated chiefly as adhering chromatin, while the bulk of nuclear material is absent. Apparently all membranes are disrupted by the detergent, and potential membrane functions such as active Ca^{++} transport will be absent in isolated preparations. Consequently nothing related to possible spindle-membrane interactions can be studied in isolates. For example, the surface of reconstituting daughter nuclei in telophase spindles will not be covered with any reforming nuclear membranes (Figures 79 and 81), as might be the case in situ. The absence of membranes was an advantage, since it permitted an unobscured view of the spindle framework, which is essential for SEM analysis.

That chromosome arms are not always apparent in SEM is explained by the presence of numerous microtubules closely packed around trailing chromosome arms, as illustrated in Figure 84. These microtubules would obscure chromosomes in SEM, so that in many cases not all chromosomes would be visible in SEM preparations.

The presence of a kinetochore in the isolated spindle shows that

this structure, integral to spindle assembly and function in all theories of mitosis, is preserved by TPM isolation medium. TPM-isolates may therefore prove useful for in vitro spindle assembly studies, utilizing dissociated spindle preparations containing both chromosomes with kinetochores and centriole complexes. These might function as nucleating sites under polymerizing conditions in the presence of added tubulin, such as has been done with basal bodies, flagellar axonemes and neurotubules by Rosenbaum et al. (1975). The possibility is also raised that kinetochore structure itself might be examined with SEM in a favorable preparation.

The location of reconstituting daughter nuclei at the extremities of telophase spindles may be functionally related to the many microtubules seen within the daughter nuclei at this stage (Figure 82). These microtubules might act as a framework along which nuclei move to their terminal positions.

Electron-dense midbodies are present in late anaphase spindles (Figures 79-81). Midbodies are not recognizable in SEM, although in Figure 76 a suggestion of interfibrillar material can be seen throughout much of the spindle midregion. In TEM microtubules appear to enter the midbody from both half spindles, and regularly arrayed material can sometimes be seen between adjacent microtubules within the midbody. Bridges between microtubules have been seen in spindles of other species (for example, Hepler et al., 1970), and their presence is essential for generation of force in all sliding microtubule models of chromosome movement (Subirana, 1968; McIntosh et al., 1969; Nicklas, 1971). Evidence that the one large midbody of telophase is the result of fusion of four separate smaller anaphase midbodies is shown in Figure 81, in

which the plane of section evidently passed through only the outer portion of the telophase midbody. A similar case is reported by Robbins and Gonatas (1964) in HeLa cells, when anaphase stembodies composed of overlapping ends of microtubules in an amorphous material move to the spindle midplane, where they cluster and fuse. In that system the term "midbody" refers to the interzonal microtubules and stembodies which are compressed into a narrow neck region in telophase as the plasma membrane indents. In contrast, in blastema embryos of D. melanogaster the midbodies are not directly involved in cytokinesis, as the embryo at this stage is a syncytium. The possibility remains that in Drosophila midbodies are in some fashion related to the reversible plasma membrane indentations which occur between the 10th and 11th, and between 11th and 12th divisions after fertilization (during the blastema stage), which might be similar to the conditions for midbody formation present during early cytokinesis in HeLa cells.

6. Events of the mitotic cycle

SEM reveals the progressively more ordered fibrous structure of spindles at different stages of the mitotic cycle. The relatively thin and somewhat tangled fibrils of prophase (Figures 68, 69, 70) assume a more linear arrangement in late prophase (Figure 71) and are organized into bundles at anaphase (Figures 72, 73). By telophase (Figure 76) one thick interzonal bundle remains. In metaphase and anaphase as seen in phase contrast (Figures 42, 43, 46, 47), there are a fairly small number of major fibers visible, perhaps three or four. Four midbodies, but not more, have been observed in anaphase spindles, again suggesting that there may be four major fibers involved. Since Drosophila and other Diptera exhibit the phenomenon of somatic pairing of homologues

during the mitotic cycle (Metz, 1916), there will be four pairs of chromosomes per half-spindle in D. melanogaster (2n = 8). The number of major fibers may therefore be significant, suggesting a relationship between each chromosome pair and a major non-chromosomal fiber. Trailing chromosome arms often seem associated with one of the interzonal fibers (for example, Figure 46); this could be fortuitous, however. In SEM also, trailing arms seem to be directly opposite each other and may be associated with the same interzonal fiber (Figure 75). The four interzonal fibers seen in late anaphase might serve as the spindle framework, along or inside which the four pairs of homologous chromosomes move towards the poles.

In the transition from anaphase to telophase separate interzonal fibers disappear, giving the impression that they associate laterally to form the telophase interzonal fibril bundle. In SEM the telophase interzonal bundle is about 0.9 µm thick (Figure 76), and this is sufficient to accommodate all of the anaphase interzonal fibrils if they were to associate laterally (Figure 73). Since there is no cytokinesis at the blastema stage, the presence of midbodies indicates their direct involvement in mitosis, possibly as regions of overlap between non-chromosomal microtubules of opposite polarity which have been implicated in a sliding spindle elongation mechanism (Pickett-Heaps, McDonald and Tippit, 1975).

The observed bending of telophase spindles might be significant in terms of spindle mechanics. SEM reveals an apparent twist of the interzonal fiber bundle (Figure 76), suggesting that the two half-spindles might rotate with respect to each other.

C. Possibilities for future work with this system

1. Various Drosophila strains and mutants exist in which the

chromosome number is altered (Lindsley and Grell, 1967). These can be used for examination of the proposed correlation between haploid chromosome number and the number of interzonal fibers in anaphase spindles. The same type of material could be used to see if there is a correlation between chromosome size and interzonal fiber dimensions. During the course of this work three anaphase interzonal fibers were seen in some cases, suggesting a possible relationship between fiber size, and thus its visibility, and chromosome size. According to classical light microscopists there are three pairs of large chromosomes and one small dot-like pair in D. melanogaster.

2. Serial cross sections through isolated anaphase spindles should reveal the number of microtubules per spindle, as well as the number in each non-chromosomal spindle fiber. Such work would possibly lend support to a sliding microtubule hypothesis of chromosome movement.

3. Stereo-pair images of spindles in SEM would greatly increase the amount of information about spindle three dimensional structure which can be obtained with this method.

4. Centriole complexes are probably present in the polar regions isolated from cooled embryos (Figure 54). The study of these structures with SEM and TEM should prove fruitful. They should also be tested for their ability to act as MTOC's by incubation under polymerizing conditions in a tubulin-containing medium, as Rosenbaum et al. (1975) did with other MTOC's.

V. Summary

Mitotic spindles of D. melanogaster embryos in situ are surrounded by multiple layers of membranes which have been termed spindle-delimiting membranes. These membranes, in conjunction with tubular ER present at spindle poles, may function in controlling Ca^{++} levels and therefore microtubule assembly in vivo.

Spindles can easily be isolated, using either a hexylene glycol isolation medium or a low Ca^{++} tubulin polymerizing medium (TPM). TPM-isolates preserve major in situ characteristics of spindles, and therefore were selected for further study (below).

In phase contrast, four major interzonal spindle fibers are visible. This may be significant since D. melanogaster has four pairs of chromosomes. Each interzonal fiber has a midbody at its midregion. At telophase the four midbodies of anaphase apparently coalesce (laterally) into one large midbody, and only one broad interzonal fiber can be seen.

The scanning electron microscope (SEM) was used for part of this study. Methods were developed for following the fate of individual spindles through all steps of prcessing for the SEM. The SEM shows a progressively more ordered spindle framework developing from prophase through anaphase and telophase. Chromosomes on the spindle have been identified, and a centriole complex, apparently consisting of a centriole plus associated material, has been described. Larger diameter spindle fibers appear to be composed of bundles of small diameter fibrils.

Thin sections through TPM isolates verify the presence of midbodies, which are not visualized with the SEM. In this system, in which cytokinesis does not occur during this stage of development, midbodies seem not to be directly involved in cytokinesis.

APPENDIX

An estimate of the amount of tubulin in a metaphase spindle.

Previous attempts at estimating the amount of tubulin contained in a spindle from structural information alone have utilized cross sections from isolated sea urchin mitotic apparatus (Cohen and Rebhun, 1970) or from crane fly spermatocytes (Fuge, 1974). Based on the numbers of microtubules per thin section, both reports calculate approximately 10^8 monomers of tubulin per metaphase spindle (without asters) (Fuge, 1974).

With favorable specimens and SEM it is possible to estimate the amount of tubulin present in a spindle, with the added advantage that with SEM the entire spindle is visible in one micrograph, thus eliminating the major problem of spindle reconstruction from thin sections, which was necessary in earlier studies.

A flattened metaphase spindle without asters, like that shown in Figure 85, can be used for an estimation of tubulin content. Results here can be compared with those studies mentioned above, and with a calculation of the tubulin content of D. melanogaster embryos based on colchicine binding activity (Green et al., 1975).

This atypical metaphase spindle is more flattened against the coverslip than the usual metaphase spindle seen in SEM, and the majority of its fibrils appear to be visible in this micrograph because of spreading.

The number of microtubules in this spindle was estimated in the following ways. At three locations on the micrograph parallel lines were drawn perpendicular to the long axis of the spindle (Figure 85, a, b, and c). At each of these levels across the spindle two numbers were

Plate XXX. Flattened metaphase spindle in SEM.

Figure 85. Metaphase spindle, extremely flattened against the coverslip, making it useful for an estimation of the tubulin content of this spindle. At three different levels across the spindle (lines a, b, c, left and right sides of micrograph) measurements were made. SEM, X 10,000.

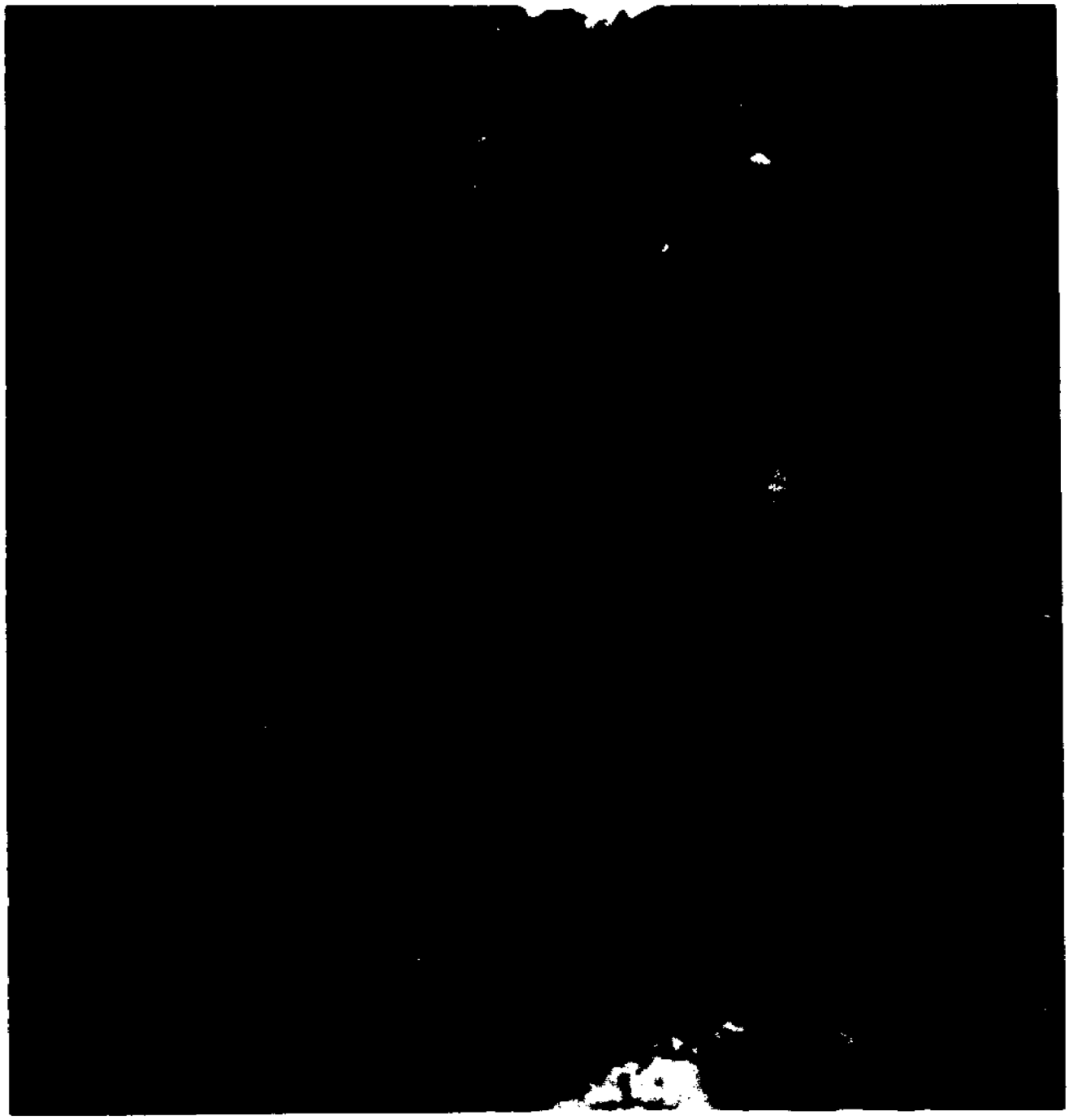

obtained: (1) a direct measurement of the total linear millimeters of fibrillar diameters, and (2) counts of size classes of fibrillar diameters.

Results of the first method of measuring were: level a, 50 mm; level b, 40 mm; and level c, 42.5 mm. For the following calculation it was assumed that the spindle is perfectly flat and uniformly one microtubule (mt) thick. Any non-microtubule material, such as clear zones around microtubules, chromosomes, and the metal coating applied for SEM, is disregarded. Each millimeter in the micrograph (10,000X) represents 100 nm of true length, and therefore could contain up to four adjacent microtubules, each 25 nm in diameter. The value obtained by this method will be a minimum estimation, since the spindle in Figure 85 is probably more than one microtubule thick.

At level a: 50 mm x 4 mt/mm = 200 mt across the spindle. (Calculations will be shown only for level a). Since this is a metaphase spindle, each microtubule will be assumed to extend from pole to pole, or 150 mm on the micrograph (actual length = 15 µm or 15,000 nm). Total length in nm of mt in the spindle, based on measurements at level a are then: 200 mt x 15,000 nm/mt = 3.0×10^6 nm/spindle

Each microtubule is assumed to be composed of 13 protofilaments, and the 6S dimer of tubulin has a molecular weight of about 110,000 daltons, so that monomers comprising the protofilaments have a molecular weight of 55,000 daltons and a diameter of about 40 A (4 nm) (Erickson, 1975).

For level a: 3.0×10^6 nm of mt/spindle x 13 protofil/mt = 39.0×10^6 nm of protofil/spindle. This figure divided by 4 nm/tubulin monomer = 9.8×10^6 monomers/spindle. This number (and results from level b: 7.8×10^6 monomers/spindle and level c: 8.4×10^6 monomers/spindle) is

clearly much lower than numbers obtained by Cohen and Rebhun (1970) and Fuge (1974). Even if it were assumed that this spindle is two microtubules thick (rather than one), results would only be in the range of 10^7 monomers/spindle, which is still an order of magnitude lower than amounts calculated by these investigators.

For estimation of the number of grams of tubulin required to construct this spindle, and all spindles in the syncytial embryo of D. melanogaster, results at level a will again be used:

9.8×10^6 monomers/spindle x 5.5×10^4 daltons/monomer x 1.67×10^{-24} gm/dalton = 9.0×10^{-13} gm/spindle.

Up to 6500 spindles may be present by the end of the blastema divisions (Zalokar, 1976), all of which occur while the embryo is still a syncytium, so that 9.0×10^{-13} gm/spindle x 6500 spindles = 5.8×10^{-9} gm/embryo needed to construct all the spindles in the pre-blastoderm stages.

Green et al. (1975) estimate the minimum tubulin pool size in D. melanogaster during the first 5 hours after fertilization (a period which includes the blastema divisions) at 10×10^{-9} gm/embryo, which is the same order of magnitude as the minimum estimate calculated here on structural information alone.

In the second method used to estimate numbers of microtubules, it was assumed that the spindle is composed of microtubule bundles which are cylindrical, and whose diameter is proportional to the number of microtubules contained in the bundle. Fibrils were measured and classified into these groups:

Level	Fibril diameter				
	less than 100 nm	approx. 100 nm	approx. 150 nm	approx. 250 nm	greater than 250 nm
a	18	10	6	4	0
b	8	3	2	9	2
c	29	12	4	2	0

Assumed average # mt/fibril diameter:

2	4	6	10	12

mt/fibril = πr^2, and r = $\frac{1}{2}$ # mt/fibril diameter

	π	4π	9π	25π	36π
a	18π	40π	54π	100π	0
b	8π	12π	18π	225π	72π
c	29π	48π	36π	50π	0

Total # of mt at each level:

Level a 512

b 1052

c 666

By this second method, numbers of microtubules are estimated at 3 - 6 times greater than by the first method, or, for level a: 2.5×10^7 monomers/spindle and 1.5×10^{-8} gm of tubulin/embryo. This data is in good agreement with that published for both numbers of monomers/spindle in other species and numbers of grams of tubulin per embryo in D. melanogaster.

Estimation of microtubule numbers here would be greatly improved

through use of stereo pairs of micrographs of such spindles, providing more accurate information concerning fibril bundle shape (cylindrical versus flattened) and the presence and position of chromosomes. Therefore, this calculation is advanced as a tentative estimation, but one which shows the potential use of the methods here developed.

Additional data is provided by the second set of estimated numbers of microtubules. The number of microtubules at level b, spindle mid-region, is approximately twice the number of microtubules estimated either at level a or c, suggesting that microtubules may overlap in the middle of the spindle and thus may be able to slide relative to each other.

BIBLIOGRAPHY

Anderson, T.F. 1951. Techniques for the preservation of three-dimensional structure in preparing specimens for the electron microscope. Trans. N.Y. Acad. Sci. 13: 130-134.

Bajer, A. 1973. Interaction of microtubules and the mechanism of chromosome movement (zipper hypothesis) I. General principal. Cytobios 8: 139-160.

Bajer, A. and Molé-Bajer, J. 1969. Formation of spindle fibers, kinetochore orientation, and behavior of the nuclear envelope during mitosis in endosperm. Fine structural and in vitro studies. Chromosoma (Berl.) 27: 448-484

Behnke, O. and Forer, A. 1966. Some aspects of microtubules in spermatocyte meiosis in a crane fly (Nephrotoma suturalis Loew): intranuclear and intrachromosomal microtubules. C.r. Lab. Carlsberg 35: 437-455.

Brinkley, B.R. and Cartwright, Jr., J. 1971. Ultrastructural analysis of mitotic spindle elongation in mammalian cells in vitro. J. Cell Biol. 50: 416-431

Brinkley, B.R. and Stubblefield, E. 1970. Ultrastructure and interaction of the kinetochore and centriole in mitosis and meiosis. In Advances in Cell Biology. Eds. Prescott, D.M., Goldstein, L. and McConkey, E. Appleton-Century-Crofts, Inc., New York, N.Y.

Cande, W.Z., Snyder, J., Smith, D., Summers, K. and McIntosh, J.R. 1974. A functional mitotic spindle prepared from mammalian cells in culture. Proc. Nat. Acad. Sci. USA 71: 1559-1563.

Chang, J.P. 1971. A new technique for separation of coverglass substrate from epoxy-embedded specimens for electron microscopy. J. Ultrastruc. Res. 37: 370-377.

Cohen, W.D. 1968. Polyelectrolyte properties of the isolated mitotic apparatus. Exptl. Cell Res. 51: 221-236.

Cohen, W.D. and Gottlieb, T. 1971. C-microtubules in isolated mitotic spindles. J. Cell Sci. 9: 603-619.

Cohen, A.L., Marlow, D.P., and Garner, G.E. 1968. A rapid critical point method using fluorocarbons ("Freons") as intermediate and transitional fluids. J. Microscopie 7: 331-342.

Cohen, W.D. and Rebhun, L.I. 1970. An estimate of the amount of microtubule protein in the isolated mitotic apparatus. J. Cell Sci. 6: 159-176.

Dawes, C.J. 1971. In Biological Techniques in Electron Microscopy. Barnes & Noble, Inc., New York, N.Y.

de Harven, E. 1968. The centriole and the mitotic spindle. In The Nucleus. Academic Press Inc., New York.

Ebashi, S. and Endo, M. 1968. Calcium ion and muscle contraction. Prog. Biophys. Mol. Biol. 18: 125-183.

Ephrussi, B. and Beadle, G.W. 1936. A technique of transplantation for Drosophila. Am. Naturalist 70: 218-225.

Erickson, H.P. 1975. The structure and assembly of microtubules. Ann. N.Y. Acad. Sci. 253: 60-77.

Fausto-Sterling, A., Zheutlin, L.M. and Brown, P.R. 1974. Rates of RNA synthesis during early embryogenesis in Drosophila melanogaster. Devel. Biol. 40: 78-83.

Fawcett, D.W. 1961. Intercellular bridges. Exptl. Cell Res., Suppl. 8: 174-187.

Forer, A. 1966. Characterization of the mitotic traction system, and evidence that birefringent spindle fibers neither produce nor transmit force for chromosome movement. Chromosoma (Berl.) 19: 44-98.

Forer, A. 1969. Chromosome movements during cell-division. In Handbook of Molecular Cytology. A. Lima-de-Faria, Ed.: 553-601. North-Holland Publishing Company. Amsterdam, Holland and London, England.

Forer, A. 1974. Possible roles of microtubules and actin-like filaments during cell-division. In Cell Cycle Controls. G.M. Padilla, I.L. Cameron and A. Zimmerman, Eds.: 319-336. Academic Press Inc., New York, N.Y.

Forer, A. and Goldman, R.D. 1972. The concentrations of dry matter in mitotic apparatuses in vivo and after isolation from sea-urchin zygotes. J. Cell Sci. 10: 387-418.

Forer, A. and Zimmerman, A.M. 1974. Characteristics of sea-urchin mitotic apparatus isolated using a dimethyl sulfoxide/glycerol medium. J. Cell Sci. 16: 481-497.

Fritz-Niggli, H. and Suda, T. 1972. Bildung and Bedeutung der Zentriolen: Eine Studie und Neuinterpretation der Meiose von Drosophila. Cytobiologie 5: 12-41.

Fuge, H. 1973. Verteilung der Mikrontubuli in Metaphase-und Anaphase-Spindeln der Spermatocyten von Pales ferruginea. Eine quantitative Analyse von Serienquerschnitten. Chromosoma (Berl.) 43: 109-143.

Fuge, H. 1974. An estimation of the microtubule content of crane fly spindles based on microtubule counts. Protoplasma 79: 391-393.

Fuller, G.M., Artus, C.S. and Ellison, J.J. 1976. Calcium as a regulator of cytoplasmic microtubule assembly and disassembly. J. Cell Biol. 70: 68a.

Fullilove, S.L. and Jacobson, A.G. 1971. Nuclear elongation and cytokinesis in Drosophila montana. Devel. Biol. 26: 560-577.

Fulton, C. 1971. Centrioles. In Origin and Continuity of Cell Organelles. J. Reinert and H. Ursprung, Eds.: 170-221. Springer-Verlag New York, Heidelberg, Berlin.

Gallin, J.I. and Rosenthal, A.S. 1974). The regulatory role of divalent cations in human granulocyte chemotaxis. J. Cell Biol. 62: 594-609.

Goldman, R.D. and Rebhun, L.I. 1969. The structure and some properties of the isolated mitotic apparatus. J. Cell Sci. 4: 179-209.

Green, L.H., Brandis, J.W., Turner, F.R. and Raff, R.A. 1975. Cytoplasmic microtubule proteins of the embryo of Drosophila melanogaster. Biochemistry 14: 4487-4491.

Harris, P. 1962. Some structural aspects of the mitotic apparatus in sea urchin embryos. J. Cell Biol. 14: 475-487.

Hepler, P.K., McIntosh, J.R. and Cleland, S. 1970. Intermicrotubule bridges in mitotic spindle apparatus. J. Cell Biol. 45: 438-444.

Hill, D.L. 1945. Chemical removal of the chorion from Drosophila eggs. D.I.S. 19: 62.

Hoage, T.R. and Kessel, R.G. 1968. An electron microscope study of the process of differentiation during spermatogenesis in the drone honey bee (Apis mellifera L.) with special reference to centriole replication and elimination. J. Ultrastruct. Res. 24: 6-32.

Hoffman-Berling, H. 1954. Adenosintriphosphat als Betriebsstoff von Zellbewegungen. Biochim. Biophys. Acta 14: 182-194.

Huettner, A.F. 1933. Continuity of the centrioles in Drosophila melanogaster. Z.f. Zellforschung. u. mikr. Anatomie 19: 119-134.

Inoué, S. 1960. On the physical properties of the mitotic spindle. Ann N.Y. Acad. Sci. 90: 529.

Inoué, S., Borisy, G.G. and Kiehart, D.P. 1974. Growth and lability of Chaetopterus oocyte mitotic spindles isolated in the presence of porcine brain tubulin. J. Cell Biol. 62: 175-184.

Inoué, S. and Sato, H. 1967. Cell motility by labile association of molecules. J. Gen. Physiol. 50: 259-292.

Ito, S. 1960 . The lamellar systems of cytoplasmic membranes in dividing spermatogenic cells of Drosophila virilis. J. Biophys. Biochem. Cytol. 7: 433-442.

Kane, R.E. 1962. The mitotic apparatus: fine structure of the isolated unit. J. Cell Biol. 15: 279-287.

Kane, R.E. 1965. The mitotic apparatus: Physical-chemical factors controlling stability. J. Cell Biol. 23: 137-144.

Kane, R.E. 1967. The mitotic apparatus. Identification of the major soluble component of the glycol-isolated mitotic apparatus. J. Cell Biol. 32: 243.

Kane, R.E. and Forer, A. 1965. The mitotic apparatus. Structural changes after isolation. J. Cell Biol. 25: 31-39.

Kersey, Y.M. and Wessells, N.K. 1976. Localization of actin filaments in internodal cells of Characean algae. A scanning and transmission electron microscope study. J. Cell Biol. 68: 264-275.

Kiefer, B., Sakai, H., Solari, A.J. and Mazia, D. 1966. The molecular unit of the microtubules of the mitotic apparatus. J. molec. Biol. 20: 75-79.

Kiehart, D.P. and Inoué, S. 1976. Local depolymerization of spindle microtubules by microinjection of calcium ions. J. Cell Biol. 70: 230a.

Kinderman, N.B. and King, R.C. 1973. Oogenesis in Drosophila virilis. I. Interactions between the ring canal rims and the nucleus of the oocyte. Biol. Bull. 144: 331-354.

King, R.C. 1970. In Ovarian Development in Drosophila melanogaster. Academic Press, New York.

Kirschner, R.H., Rusli, M. and Martin, T.E. 1975. Scanning electron microscopy of isolated mouse liver nuclei. J. Cell Biol. 67: 213a.

Kubai, D.F. 1975. The evolution of the mitotic spindle. Int. Rev. Cytol. 43: 167-227.

Limbourg, B. and Zalokar, M. 1973. Permeabilization of Drosophila eggs. Devel. Biol. 35: 382-387.

Lindsley, D.L. and Grell, E.H., eds. 1967. Genetic variations of Drosophila melanogaster. Carnegie Institute of Washington, publication 627.

Luft, J.H. 1961. Improvements in epoxy embedding methods. J. Biophys. Biochem. Cytol. 9: 409-414.

Lung, B. 1974. The preparation of small particulate specimens by critical point drying: application for scanning electron microscopy. J. Microscopy 101: 77-80.

Mahowald, A.P. 1962. Fine structure of pole cells and polar granules in Drosophila melanogaster. J. Exptl. Zool. 151: 201-216.

Mahowald, A.P. 1963a. Electron microscopy of the formation of the cellular blastoderm in Drosophila melanogaster. Exptl. Cell Res. 32: 457-468.

Mahowald, A.P. 1963b. Ultrastructural differentiations during formation of the blastoderm in the Drosophila melanogaster embryo. Devel. Biol. 8: 186-204.

Mazia, D. and Dan, K. 1952. The isolation and biochemical characterization of the mitotic apparatus of dividing cells. Proc. Nat. Acad. Sci. USA 38: 826-838.

Mazia, D., Mitchison, J.M., Medina, H. and Harris, P. 1961. The direct isolation of the mitotic apparatus. J. Biophys. Biochem. Cytol. 10: 467-474.

Mazia, D., Petzelt, C., Williams, R.O. and Meza, I. 1972. A Ca-activated ATPase in the mitotic apparatus of the sea urchin egg (isolated by a new method). Exptl. Cell Res. 70: 325-332.

Mazia, D., Schatten, G. and Sale, W. 1975. Adhesion of cells to surfaces coated with polylysine. Applications to electron microscopy. J. Cell Biol. 66: 198-200.

McIntosh, J.R., Cande, Z., Snyder, J. and Vanderslice, K. 1975. Studies on the mechanism of mitosis. Ann. N.Y. Acad. Sci. 253: 407-427.

McIntosh, J.R., Hepler, P.K. and Van Wie, D.G. 1969. Model for mitosis. Nature 224: 659-663.

McIntosh, J.R., and Landis, S.C. 1971. The distribution of spindle microtubules during mitosis in cultured human cells. J. Cell Biol. 49: 468-497.

Metz, C.W. 1916. Chromosome studies in the Diptera. II. The paired association of chromosomes in the Diptera, and its significance. J. Exp. Zool. 21: 213-280.

Metz, C.W. 1926. Observations on spermatogenesis in Drosophila. Z. Zellforsch. u. Mikr. Anat. 4: 1-28.

Milsted, A. and Cohen, W.D. 1973. Mitotic spindles from Drosophila melanogaster. Exptl. Cell Res. 78: 243-246.

Milsted, A., Cohen, W.D. and Lampen, N. 1976. Mitotic spindles of Drosophila melanogaster: a phase contrast and scanning electron microscope study. J. Cell Sci. in press.

Mossige, J.C. 1966. Fermented yeast for egg collection. D.I.S. 41: 187.

Muller, W. 1970. Interferenzmikroskopische Untersuchungen der Trockenmassenkonzentration in isolierten Mitoseapparaten und lebenden Spermatocyten von Pales ferruginea (Nematocera). Chromosoma (Berl.) 30: 305-316.

Müller, W. 1972. Elektronenmikroskopische Untersuchungen zum Formwechsel der Kinetochoren wahrend der Spermatocytenteilungen von Pales ferruginea (Nematocera). Chromosoma (Berl.) 38: 139-172.

Nicklas, R.B. 1971. Mitosis. In Advances in Cell Biology. Vol. 2. D.M. Prescott, L. Goldstein and E.H. McConkey, eds.: 225-279. Appleton-Century-Crofts, Inc., New York, N.Y.

Okada, E. and Waddington, C.H. 1959. The submicroscopic structure of the Drosophila egg. J. Embryol. Exptl. Morphol. 7: 583-597.

Paweletz, N. 1967. Zur Funktion der "Fleming-korpus" bei der Teiling tierisches Zellen. Naturwissenschaften 54: 533-535.

Pickett-Heaps, J.D. 1969. The evolution of the mitotic apparatus: an attempt at comparative ultrastructural cytology in dividing plant cells. Cytobios 1: 257-280.

Pickett-Heaps, J.D., McDonald, K.L. and Tippitt, D.H. 1975. Spindle structure and function in diatoms. J. Cell Biol. 67: 336a.

Rabinowitz, M. 1941. Studies on the cytology of the egg of Drosophila melanogaster. J. Morphology 69: 1-49.

Rebhun, L.I. 1967. Structural aspects of saltatory particle movement. J. Gen. Physiol. 50: 223-239.

Rebhun, L.I., Jemiolo, D., Ivy, N., Mellon, M., and Nath, J. 1975. Regulation of the in vivo mitotic apparatus by glycols and metabolic inhibitors. Ann. N.Y. Acad. Sci. 253: 362-377.

Rebhun, L.I., Rosenbaum, J., Lefebvre, P. and Smith, G. 1974. Reversible restoration of the birefringence of cold-treated, isolated mitotic apparatus of surf clam eggs with chick brain tubulin. Nature 249: 113-115.

Rebhun, L.I. and Sander, G. 1967. Ultrastructure and birefringence of the isolated mitotic apparatus of marine eggs. J. Cell Biol. 34: 859-883.

Rebhun, L.I. and Sharpless, T.K. 1964. Isolation of spindles from the surf clam Spisula solidissima. J. Cell Biol. 22: 488-491.

Reynolds, E.S. 1963. The use of lead citrate at high pH as an electron-opaque stain in electron microscopy. J. Cell Biol. 17: 208-212.

Robbins, E. and Gonatas, N.K. 1964. The ultrastructure of a mammalian cell during the mitotic cycle. J. Cell Biol. 21: 429-463.

Robbins, E. and Jentzch, G. 1969. Ultrastructural changes in the mitotic apparatus at the metaphase to anaphase transition. J. Cell Biol. 40: 678-691.

Rosenbaum, J.L., Binder, L.I., Granett, S., Dentler, W.L., Snell, W., Sloboda, R. and Haimo, L. 1975. Directionality and rate of assembly of chick brain tubulin onto pieces of neurotubules, flagellar axonemes, and basal bodies. Ann. N.Y. Acad. Sci. 253: 147-177.

Roth, L.E. and Daniels, E.W. 1962. Electron microscopic studies of mitosis in amebae. II. The giant amebae Pelomyxa carolinensis. J. Cell Biol. 12: 57-78.

Sakai, H. 1966. Studies on sulfhydryl groups during cell divisions of sea-urchin eggs. VIII. Some properties of mitotic apparatus proteins. Biochem. biophys. Acta 112: 132-145.

Salmon, E.D. 1975. Spindle microtubules: thermodynamics of in vivo assembly and role in chromosome movement. Ann. N.Y. Acad. Sci. 253: 383-406.

Sayles, C.D., Procunier, J.D. and Browder, L.W. 1973. Radiolabelling of Drosophila embryos. Nature New Biol. 241: 215-216.

Schliwa, M. 1976. The role of divalent cations in the regulation of microtubule assembly. In vivo studies on microtubules of the heliozoan axopodium using the ionophore A23187. J. Cell Biol. 70: 527-540.

Schneider, I. 1972. Cell lines derived from late embryonic stages of Drosophila melanogaster. J. Embryol. exp. Morph. 27: 353-365.

Schrader, F. 1953. Mitosis. The movements of chromosomes in cell division. Columbia University Press, New York.

Sisken, J.E., Wilkes, E., Donnelly, G.M. and Kakefuda, T. 1967. The isolation of the mitotic apparatus from mammalian cells in culture. J. Cell Biol. 32: 212-216.

Sonnenblick, B.P. 1950. In Biology of Drosophila. M. Demerec, ed.: 62-167. John Wiley & Sons, Inc., New York.

Spurlock, B.O., Skinner, M.S. and Kattine, A.A. 1966. A simple rapid method for staining epoxy-embedded specimens for light microscopy with the polychromatic stain Paragon-1301. Amer. J. Clin. Pathol. 46: 252-257.

Subirana, J.A. 1968. Role of spindle microtubules in mitosis. J. Theoret. Biol. 20: 117-123.

Szollosi, D. 1964. The structure and function of centrioles and their satellites in the jellyfish Phialidium gregarium. J. Cell Biol. 21: 465-479.

Taylor, E.W. 1975. Conference summary. Ann. N.Y. Acad. Sci. 253: 797-802.

Tippit, D.H., McDonald, K.L. and Pickett-Heaps, J.D. 1975. Cell division in the centric diatom Melosira varians. Cytobiologie 12: 52-73.

Vial, J. and Porter, K.R. 1975. Scanning electron microscopy of dissociated tissue cells. J. Cell Biol. 67: 345-360.

Watson, M.L. 1958. Staining of tissue sections for electron microscopy with heavy metals. J. biophys. Biochem. Cytol. 4: 475-478.

Weisenberg, R.C. 1972. Microtubule formation in vitro in solutions containing low calcium concentrations. Science 177: 1104-1105.

Widmer, B. and Gehring, W.J. 1974. A method for permeabilization of Drosophila eggs. D.I.S. 51: 149.

Zalokar, M. 1971. Fixation of Drosophila eggs without pricking. D.I.S. 47: 128-129.

Zalokar, M. 1976. Autoradiographic study of protein and RNA formation during early development of Drosophila eggs. Devel. Biol. 49: 425-437.

Zamboni, L. and Gondos, B. 1968. Intercellular bridges and synchronization of germ cell differentiation during oogenesis in the rabbit. J. Cell Biol. 36: 276-282.